ORIGINAL RESEARCH

Physiologia Plantarum

Volatilome and proteome responses to *Colletotrichum lindemuthianum* infection in a moderately resistant and a susceptible bean genotype

Maurilia M. Monti[1] | Ilaria Mancini[2] | Liberata Gualtieri[1] | Guido Domingo[2] | Marzia Beccaccioli[3] | Rosanna Bossa[4] | Marcella Bracale[2] | Francesco Loreto[1,4] | Michelina Ruocco[1]

[1]Istituto per la Protezione Sostenibile delle Piante, CNR, Portici, Napoli, Italy

[2]Dipartimento di Biotecnologie e Scienze della Vita, Università degli Studi dell'Insubria, Varese, Italy

[3]Dipartimento di Biologia Ambientale, Università Sapienza Roma, Roma, Italy

[4]Dipartimento di Biologia, Università degli Studi di Napoli Federico II, Naples, Italy

Correspondence
Guido Domingo, Dipartimento di Biotecnologie e Scienze della Vita, Università degli Studi dell'Insubria, via J.H. Dunant 3, I-21100 Varese, Italy.
Email: g.domingo@uninsubria.it

Maurilia M. Monti, Istituto per la Protezione Sostenibile delle Piante, CNR, Piazzale E. Fermi 1, I-80055 Portici, Naples, Italy.
Email: mauriliamaria.monti@cnr.it

Abstract

We analyzed the changes in the volatilome, proteome, stomatal conductance, salicylic and jasmonic acid contents of a susceptible and a moderately resistant genotype of common bean, *Phaseoulus vulgaris* L., challenged with *Colletotrichum lindemuthianum*, the causal agent of fungal anthracnose. Our results indicate differences at both proteome and volatilome levels between the two genotypes, before and after the infection, and different defense strategies. The moderately resistant genotype hindered pathogen infection, invasion, and replication mainly by maintaining epidermal and cell wall structure. The susceptible genotype was not able to limit the early stages of pathogen infection. Rather, stomatal conductance increased in the infected susceptible genotype, and enhanced synthesis of Green Leaf Volatiles and salicylic acid was observed, together with a strong hypersensitive response. Proteomic investigation provided a general framework for physiological changes, whereas observed variations in the volatilome suggested that volatile organic compounds may principally represent stress markers rather than defensive compounds per se.

1 | INTRODUCTION

Common bean (*Phaseolus vulgaris* L.) is an important staple crop worldwide, with high nutritional value in terms of proteins, minerals, and fibers. Beans are the primary source of protein for humans in many developing countries (Castro-Guerrero et al., 2016; Myers & Kmiecik, 2017; Rendón-Anaya et al., 2017). The production, yield and quality of beans are affected by many pathogens, among which fungal

anthracnose is one of the most destructive, causing up to 90% potential yield losses, especially under cool and humid environmental conditions (Bardas et al., 2009; Sharma et al., 2008). The causal agent of anthracnose is the fungus *Colletotrichum lindemuthianum* (Sacc. & Magnus), a hemibiotrophic pathogen that can be transmitted via infested seeds or soil. *C. lindemuthianum* conidia can be dispersed by wind and rainfall and can also germinate on the leaf surface to directly infect the aerial parts of the plant. Upon entering the plant,

C. lindemuthianum first establishes a biotrophic infection and subsequently switches to the necrotrophic phase. Induced cell death generates phenotypically visible disease symptoms in the form of necrotic lesions on stems, leaves, pods, and seeds (Mohammed, 2013).

C. lindemuthianum is a highly variable pathogen resulting in many physiological races. During bean-*C. lindemuthianum* coevolution, the pathogen evolved a great pathogenic variability, making most of the cultivated varieties susceptible, though with intraspecific variability. To date, more than 298 races of the pathogen have been identified worldwide (Nunes et al., 2021) and it has been verified that the resistance of most bean cultivars follows the gene-for-gene (R/Avr) model, also known as race-specific resistance (Flor, 1955). Most recently, Mungalu et al. (2020) identified 14 quantitative trait loci (QTL) for resistance to nine races of *C. lindemuthianum*.

Plant-pathogen interactions are driven by an intense molecular "dialogue" between the two organisms, aiming at each one survival. Besides r-gene-mediated race-specific resistance, plants possess an innate immune system that senses herbivore- or pathogen-associated molecular patterns (HAMPs/PAMPs), in turn activating secondary signals and generating pattern-triggered immunity (PTI) (Jones & Dangl, 2006). In addition, upon damage, plants recognize endogenous molecules like self-DNA as damage-associated molecular patterns (DAMPs), recently reviewed by Tanaka and Heil (2021). During the initial phase of PTI, DAMPs, HAMPs, and PAMPs trigger conserved early secondary signals, such as reactive oxygen species (ROS) and mitogen-activated protein kinases (MAPKs) (Albert et al., 2020; Boller & Felix, 2009; Fichman & Mittler, 2020; Hou et al., 2019). Subsequently, enemy-specific responses are orchestrated by hormones such as ethylene (ET), jasmonic acid (JA), and salicylic acid (SA). In most cases, chewing herbivores and necrotrophic pathogens trigger a JA-dependent "wound response," while sap-sucking insects and biotrophic pathogens trigger a SA-dependent "systemic acquired resistance" (SAR), which usually is characterized by the induction of a hypersensitive reaction (HR) and pathogenesis-related (PR) proteins with direct antimicrobial activities such as chitinases and glucanases (Campos et al., 2014; Ding & Ding, 2020; Klessig et al., 2018; Pieterse et al., 2012). The two responses are controlled by SA and JA and are frequently subjected to a negative trade-off, with the consequence that hemibiotrophic pathogens represent notoriously difficult cases for plants to control. An analysis of the transcriptomic response of common bean to *C. lindemuthianum* infection reported an upregulation of cytokinin and ET responses, while JA, gibberellin, and abscisic acid responses were down-regulated (Oblessuc et al., 2012). However, several studies reported that treatments with PAMP-mimic compounds (such as chitosan) or with benzothiadiazole (BTH), a chemical analogue of SA, or with SA itself, induced resistance in common bean to pathogens, including *C. lindemuthianum* (Bigirimana & Höfte, 2002; De Meyer et al., 1999; Di Piero & Garda, 2008; Iriti & Faoro, 2003; Quintana-Rodriguez et al., 2015; Siegrist et al., 2000).

A fraction of the carbon assimilated by plants is emitted back into the atmosphere as volatile organic compounds (VOCs). Albeit generally small (less than 1%–2% of photosynthesis), such release of hydrocarbons has important consequences for plants and the atmosphere. VOC release is constitutive but can also be induced by abiotic and biotic stresses, for example, light, temperature, drought, salinity (Goh et al., 2016; Loreto et al., 2006; Loreto & Schnitzler, 2010), herbivores (Baldassarre et al., 2015; Heil, 2014; Kalske et al., 2019), and pathogens (Cellini et al., 2018; Ghosh et al., 2019), often acting in combination (Copolovici et al., 2014; Li et al., 2019). In all cases, VOCs seem to help plant self-defense through a range of molecular and physiological mechanisms that are not fully elucidated. Interest in using VOCs as a sustainable defense strategy with applications in agro-ecology is rising (Brilli et al., 2019). Production and roles of plant VOCs in response to mechanical wounding by herbivores have been extensively investigated for many cultivated species (Bricchi et al., 2010; Coppola et al., 2017; Portillo-Estrada et al., 2021). Hundreds of examples of direct interactions between plants and their host insects have been described, where VOCs act either as repellents or as attractive cues (Holopainen & Gershenzon, 2010). VOCs may also contribute to plant-pathogen dialogues. Studies reported that common bean and lima bean (*Phaseolus lunatus*) plants exhibit primed resistance to pathogens, including *C. lindemuthianum*, after exposure to VOCs emitted by infected conspecific plants (Girón-Calva et al., 2012; Quintana-Rodriguez et al., 2015; Yi et al., 2009), similarly as reported earlier for the induction of JA-dependent resistance responses in bean by diverse VOCs (Heil & Bueno, 2007; Jewell & Tanaka, 2019). In particular, two individual VOCs (nonanal and MeSA) primed the expression of PR proteins (Quintana-Rodriguez et al., 2015). The induction of JA-dependent resistance responses in bean by diverse VOCs was also reported (Heil & Bueno, 2007; Heil & Kost, 2006; Jewell & Tanaka, 2019; Kost & Heil, 2006; Tanaka & Heil, 2021). Moreover, many VOCs that are emitted from infected resistant plants exert direct antifungal effects and their absorbance to plant surfaces has been discussed as an additional mechanism of VOC-mediated phenotypic resistance (Camacho-Coronel et al., 2020; Quintana-Rodriguez et al., 2018). Very recently, the terpenoid volatile (E)-nerolidol has been recognized as inducer of defenses both against insects (*Empoasca onukii*) and the pathogen *Colletotrichum fructicola* in tea plants (Chen et al., 2020).

To date, few proteomic data on bean-*Colletotrichum* pathosystem have been reported. Borges et al. (2015), by using two-dimensional electrophoresis coupled with mass spectrometry, detected differentially accumulated proteins (DAPs) in inoculated leaves of *Colletotrichum*-resistant bean plants related to photosynthesis, carbon metabolism, antioxidant systems, defense and stress response, chaperones and folding catalysts, and phenylpropanoid or flavonoid biosynthesis.

All available evidence indicates that JA- and SA-dependent components of classical PTI could contribute significantly to the resistance of bean to *C. lindemuthianum*. Nevertheless, most of the research on this topic has been performed by using targeted approaches, that is, focused on molecules and genes that a priori were likely to play a role

in this context (Campa et al., 2009, 2017; Kelly & Vallejo, 2004; Sicard et al., 1997).

In the present study, we used two common bean genotypes with different levels of resistance to *C. lindemuthianum* isolate 1088 in a non-targeted comparative approach to examine physiological changes following the infection and identify VOCs and proteins that are likely to contribute to plant resistance to the infection.

2 | MATERIALS AND METHODS

2.1 | Plant material and treatments

We selected two genotypes of bean (*Phaseolus vulgaris* L.) with different levels of resistance to anthracnose, and for which earlier studies reported an inducible phenotypic response. Seeds of the commercial cultivar Flor de Junio Marcela (FJM) and the landrace Negro San Luis (NSL), as well as *C. lindemuthianum* isolate 1088 spore stock, were obtained from the Departemento de Ingenieria Genética CINVESTAV – Unidad Irapuato, GTO Mexico. While FJM exhibits a moderate level of resistance to *C. lindemuthianum*, the NSL landrace is highly susceptible to the fungal infection (Castellanos-Ramos et al., 2003; Quintana-Rodriguez et al., 2015). From now on, we use (R) to refer to the moderately resistant FJM and (S) to refer to the susceptible NSL genotype.

The conidial suspension of *C. lindemuthianum* was prepared as described by Quintana-Rodriguez et al. (2015) and suspended in distilled water with 0.1% Tween (Sigma), adjusting concentration to 1×10^7 conidia mL^{-1} by using a Burker counting chamber.

Seeds were sterilized in 1% bleach solution for 20 min, washed five times with sterile distilled water and stored on a sterile wet paper sheet at room temperature in the dark until primary root emersion (3 days). Once germinated, seeds were immersed in *C. lindemuthianum* conidial suspension for 5 min and then sowed in non-sterile commercial soil. Four seeds were sown in each pot, for a total of 20 plants per condition: susceptible not infected (S$^-$), susceptible infected (S$^+$), resistant not infected (R$^-$) and resistant infected (R$^+$). To avoid any possible airborne interaction, plants of the four treatments were grown in separate rooms of the greenhouse at $25 \pm 2°C$ and under 16 h light/8 h dark photoperiod for 21 days after sowing (DAS). At that time, disease severity was visually assessed by counting necrotic lesions.

2.2 | Plant VOC measurements

All the measurements of VOCs were performed by using a Proton Transfer Reaction-Time of Flight-Mass Spectrometer (PTR-QiToF-MS, model PTR−ToF 8000, Ionicon Analytik GmbH) with H$_3$O$^+$ as reagent ion for the proton transfer reaction (O$_2^+$ signal intensity was ca. 0.5% of the H$_3$O$^+$one). The instrument was set to a drift-tube pressure of 2.30 mbar, drift temperature of 80°C, and drift voltage of 480 V, which resulted in electric field strength to number density ratio E/N of 111 Townsend (Td, 1Td = 10–17 V cm^{-2}).

VOC measurements were performed on plants at 21 DAS. The experimental station for VOC collection consisted of two chambers, 60 cm^3 each, made of inert materials (glass and steel) and directly connected to the PTR-TOF-MS entry port. A flow of clean air (11 L min^{-1}) was generated by means of a pump (ABAC Silent LN HP2) connected to a hydrocarbon trap (Supelco Supelpure HC). The clean air flux stabilized the air background (blank) in the empty chamber. Blank measurements were performed after 30 min of continuous air flux. Then, the chambers were quickly opened, and five pots per each tested condition (S$^-$; S$^+$; R$^-$; R$^+$) were moved in and measured in each recording session separately. Head Space measurements were performed after 30 min of VOC accumulation within the chamber. Each session consisted of three 600-s-long VOC measurements. Three technical and three independent biological replicates were carried out for each condition.

2.3 | PTR-QiToF-MS data analysis

The raw data were acquired by the TOFDAQ Viewer® software (Tofwerk AG) and evaluated with the PTR-MS Viewer 3.3.8. For peak quantification, ion count rate was directly converted into a concentration unit (ppb) by using the transmission tool of the PTR-MS Viewer software. To guarantee high mass accuracy, the calibration of PTR spectra was performed on three points calibration using m/z = 21.022 (H$_3$O$^+$), m/z 330.848 (internal gas standard 1,3-diiodobenzene) and m/z = 203.943 (a fragment of 1,3-diiodobenzene). Peaks below 5 cps threshold (count per second signal from the ion detector, raw signal) were discarded as noise background.

The peaks associated with the PTR-MS ion source, including those ascribed to water chemistry or other interfering ions, for example, m/z = 32 (O$_2^+$), m/z = 31.022 (NO$^+$), m/z = 37, and m/z = 39.033 (corresponding to H$_3{}^{18}$O$^+$ and water cluster ions H$_2$O-H$_3{}^{18}$O$^+$, respectively), were removed. Blank measurements on the empty system were run before every experiment and used for background subtraction. After blank subtraction, concentration values (ppb, 10^{-9}) were normalized on fresh plant weights (FW). After filtering, 69 mass peaks were obtained, on which statistical analysis was performed.

2.4 | VOC statistical analysis

Samples normalization and all statistical analyses were carried out on Metaboanalyst online platform (Chong et al., 2018). Before statistical analysis, data were transformed with Log$_{10}$ function and auto-scaled. Principal component analysis (PCA) was carried out for the initial exploration of the data set, ensuring an objective and unsupervised analysis. Normality and homogeneity of variances were tested by using IBM SPSS Statistics (Version 27.0) before performing a two-way analysis of variance (ANOVA). Tukey's test for multiple comparisons was performed on VOC data to identify significant differences ($p < 0.05$) and to examine the influence of the two different

categorical independent variables (genotype G, and *Colletotrichum* infection C) and their interaction (I) on VOC emission. To better visualize results, hierarchical clustering of statistically differently emitted VOCs was performed (distance measure using Euclidean, and clustering algorithm using Ward D.) and visualized as heatmap.

2.5 | Gas exchange and stomatal conductance analysis

Gas exchanges were measured on fully developed and intact leaves using a portable gas exchange system GFS-3000 (Walz). The used system allows to operate with complete control of gas concentrations, incident light intensity (PAR), air temperature and relative humidity inside the cuvette. Measurements of water exchange between leaf and air were performed in vivo on three leaves for each plant exposed for 20 min to an incident PAR intensity of 500 µmol m^{-2} s^{-1}, a CO_2 flux of 400 ppm, a relative humidity of 50%, while the leaf temperature was set at 30°C. Stomatal conductance (gH_2O) was then calculated according to von Caemmerer and Farquhar (1981).

For statistical data analysis of leaf gas-exchange measurements, the SigmaPlot 14.5 software (SPSS Inc.) was used. Significance of differences between sets of data was checked by ANOVA with post-hoc Tukey test.

2.6 | Extraction and analysis of salicylic acid and jasmonic acid precursors

Analysis of SA, oxylipins and fatty acids (precursors of JA) was performed as reported previously (Beccaccioli et al., 2021) by grinding 20 mg of lyophilized bean leaves in liquid nitrogen and extracting with 750 µL of methanol–water–acetic acid (90:9:1, v/v/v) in presence of the internal standard 1-naphthaleneacetic acid (NAA MW 186.21 g mol^{-1}; at final concentration of 5 µM). Extraction was repeated and the supernatant was collected and dried by nitrogen flow. The extract was resuspended in 100 µL of water–acetonitrile (85:15, v/v) and 0.05% of acetic acid. Analysis was conducted by HPLC-MS/MS Agilent 6420 (Agilent Technologies) and chromatographic separation was performed with a Zorbax ECLIPSE XDB-C18 rapid resolution HT 4.6 × 50 mm 1.8 µm p.s. column (Agilent Technologies) at room temperature; 10 µL of extract were analyzed. The chromatographic separation was performed in presence of the mobile phases (A: water/acetonitrile 97:3 v/v containing 0.1% formic acid; B: acetonitrile/isopropyl alcohol 90:10 v/v).

For SA, the elution gradient was: 0–3 min 15% B, 3–5 min 100% B, 5–6 min 100% B, 6–7 min 15% B, and 7–8 min 15% B. The gradient was followed by 5 min (15% B) for re-equilibration. The constant flow-rate was 0.6 mL min^{-1}. The column temperature was set at 25°C.

For the oxylipins (13-hydroperoxy-9,11-octadecadienoic acid—13-HpODE-, 13-hydroxy-9,11,15-octadecatrienoic acid—13-HOTrE-, and 13-hydroxyoctadecadienoic acid—13-HODE) and fatty acids

(linoleic acid—C18:2- and gamma linolenic acid—C18:3), the elution gradient was: 0–2 min 80% A and 20% B, 2–4 min 65% A 35% B, 4–6 min 60% A and 40% B, 6–7 min 58% A and 42%, 7–9 min 52% A and 48% B, 9–15 min 35% A and 65% B, 15–17 min 25% A and 75% B, 17–18.50 min 15% A and 85% B, 18.50–19.50 min 5% A and 95% B, 19.50–24 min 5% A and 95% B, 24–26 min 1% A and 99% B, 26–30 min 1% A and 99% B, 30–34 min 80% A and 20% B. The flow rate was: 0–24 min at 0.6 mL min^{-1}, 24–30 min at 1 mL min^{-1}, and 30–34 min at 0.6 mL min^{-1}. The column temperature was set at 50°C. Metabolites were analyzed by negative ion mode electrospray ionization (ESI); SA and oxylipins by multiple reaction monitoring (MRM); fatty acids by single ion monitoring (SIM). Characteristic SIM parameters and MRM transition are reported in Table S1.

2.7 | Protein extraction

Proteins were extracted from 0.5 g (FW) of 21-day-old leaves by SDS/phenol method (Venice et al., 2021). Briefly, leaves were ground in liquid nitrogen and homogenized with extraction buffer (0.15 M Tris – HCl pH 8.8, 1% SDS, 1 mM EDTA, 0.1 M DTT, 2 mM PMSF, 0.1 mg/mL Pefabloc, 1:1000 Protease Inhibitor). After centrifugation, 1:1 volume of phenol saturated with 0.1 M Tris-HCl was added to the supernatant phase. The phenolic phase was collected and overnight precipitated with four volumes of 0.1 M ammonium acetate in methanol at −20°C. Precipitate obtained by centrifugation at 15,000 g for 10 min at 4°C was washed twice with cold 0.1 M ammonium acetate and finally with cold 80% acetone. Pellet was dried and resuspended in 100 µL of SDS-lysis buffer (20% SDS w/w, 0.25 M Tris-HCl pH 7.5, 100 mM DTT).

The proteins were quantified by the 2-D Quant-kit (GE Healthcare). All chemicals were purchased by SIGMA. Five independent biological replicates were performed for each sample.

2.8 | Trypsin digestion

Samples (150 µg of proteins) were trypsin-digested by using FASP (Filter Aided Sample Preparation) method (Vannini et al., 2019). Briefly, protein extracts were heated for 5 min at 95°C, ten times diluted with UA buffer (8 M urea in 100 mM Tris-HCl, pH 8.0) and transferred to the Amicon Ultra-0.5 Centrifugal Filter Unit.

The denaturation buffer was replaced by washing three times with UA buffer and proteins were alkylated using 50 mM iodoacetamide in UA for 15 min at room temperature and in the dark. The excess of alkylation reagents was eliminated by washing four times with ABC buffer (50 mM NH_4HCO_3). Proteins were digested overnight at 37°C with trypsin in ABC buffer (enzyme-to-substrate of 1:100 w/w ratio). The digested peptides were eluted by centrifugation. Peptide concentrations were spectrophotometrically measured, assuming that a solution of proteins with a concentration of 1 mg/mL determines an absorbance of 1.1 at 280 nm. The peptides were finally desalted onto C18 Oasis-HLB cartridges and dried down for further analysis.

2.9 | LC-MS/MS analysis and elaboration of raw data

The tryptic peptides were analyzed in a Q-Exactive mass spectrometer as previously described (Domingo, Vannini, et al., 2023). Mass spectrometer raw files were processed by using MaxQuant V1.5.3.3, (http://www.coxdocs.org/doku.php?id=maxquant:start); annotation of proteins was obtained by searching MS/MS spectra against *Phaseolus vulgaris* L. (30,554 entries; Uniprot database downloaded December 2020). The raw data obtained as output from MaxQuant ("ProteinGroups" files) were processed for identification as described elsewhere (Paradiso et al., 2020). Protein annotation was performed using default MaxQuant parameters. A false discovery rate (FDR) of 1% was accepted for both peptide and protein identification. The mass spectrometry proteomics data were deposited in the ProteomeXchange Consortium via the PRIDE (Perez-Riverol et al., 2019) partner repository with the dataset identifier PXD025070 using the following reviewer account details: Username, reviewer_pxd025070@ebi.ac.uk Password: RR9cX8Om.

Missing values were replaced with the R package impute LCMD using the hybrid imputation method (Domingo, Marsoni, et al., 2023). Quantitative proteome analyses of the filtered data were carried out on the Perseus software platform (V1.5.8.5, ttp:// www.perseus-framework.org). The Log2-transformed Label Free Quantitation (LFQ) intensities of protein groups were normalized by centering, which involved subtracting the median LFQ intensity of the entire set of protein groups for each sample (column).

2.10 | Statistical and bioinformatic analyses of proteome changes

To analyze the proteins changes in relative abundance among treatments, the fold change ratio expressed as Log_2 FC was assessed on Perseus platform. Transformed, centered and normalized Log_2 LFQ data were subjected to both one-way and two-way ANOVA based on multiple-sample tests with an FDR cut-off of 0.05 and on the Benjamini-Hochberg correction. Two-way ANOVA was performed to directly link the influence of genotype (G), treatment (*Colletotrichum* infection, C), or the interaction between them (I) on the *P. vulgaris* proteome. Perseus software platform was also used for PCA to assess the quality of our datasets.

For the annotation of the uncharacterized proteins in *P. vulgaris* and the bioinformatic analysis, a BLAST search was made against *Arabidopsis thaliana* TAIR10 (The Arabidopsis Information Resource) protein database using the online BLAST search tool in Phytozome V12.1 (https://phytozome.jgi.doe.gov/pz/portal.html) taking as valid the hits with the highest sequence similarity (expressed in percentage) and lowest e-value with respect to the target sequence.

The AGI (Arabidopsis Gene Identifiers) codes relative to each protein and percentage of similarity were included in two-way ANOVA results. Functional classification and subcellular localization were assigned using MapMan and SUBA4 tools (https://suba.live/; Hooper et al., 2017), respectively.
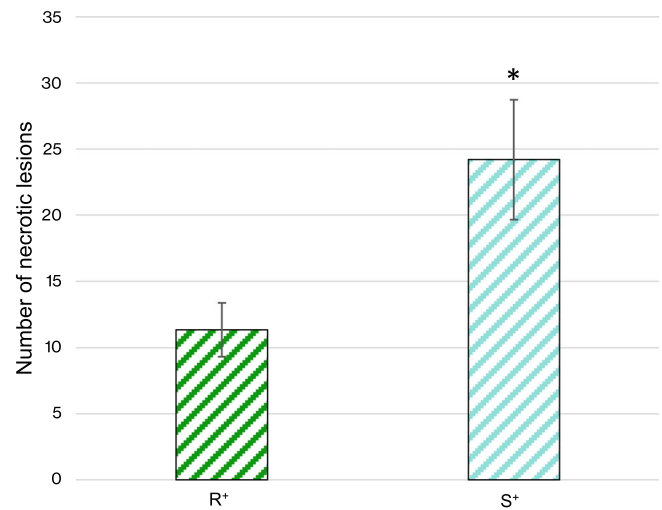

FIGURE 1 Number of necrotic lesions at 21 DAS on Flor de Junio Marcela (moderately resistant, R^+) and Negro St. Luis (susceptible, S^+) plants challenged with *Colletotrichum lindemuthianum*. Asterisk above the S^+ bar indicates significant difference with R^+ (Student's *t*-test, $p < 0.05$). Control plants not infected (R^- and S^-) are not shown, as necrotic lesions are not present.

2.11 | Protein–protein interactions network and identification of hub proteins

Using STRING (http://string-db.org/; Szklarczyk et al., 2015), a biological database and web resource for known and predicted protein–protein interactions (PPIs), we developed networks of DAPs from G-, C-, and I-lists. Parameters used included a minimum required interaction score >0.4 (medium confidence) and only connected proteins being displayed. Cytoscape software (Doncheva et al., 2018) was applied to visualize the protein interaction relationship network and identify those proteins, hereafter defined as hub proteins, with many interaction partners. After importing the data into Cytoscape and running the CytoHubba application, the top 20 proteins were evaluated by the five calculation methods (Degree, EPC, EcCentricity, MCC, and MNC). The intersecting proteins obtained using Venn plot (http://www.interactivenn.net), represent key candidates with important biological regulatory functions.

3 | RESULTS

3.1 | Disease symptoms

The first disease symptoms could be observed on the hypocotyls at 7 DAS; prior to that time, we did not observe any differences between treatments. At 21 DAS, the phenotypic disease levels of S^+ plants (quantified as the number of necrotic lesions/plant) were more than 2-fold higher than on R^+ plants (Figure 1). In particular, S^+ plants exhibited significantly more symptoms on the hypocotyls than R^+ plants. S^+ plants also exhibited visible symptoms on their primary

Flor de Junio Marcela
(FJM, moderately resistant genotype)

Negro San Luis
(NSL, susceptible genotype)

FIGURE 2 Stems and leaves of Flor de Junio Marcela (moderately resistant, R) and Negro St. Luis (susceptible, S) plants at 21 DAS. (A, B) Control plants, (C, D) plants with anthracnose symptoms on stems and leaves of Flor de Junio Marcela (A, C) and Negro St. Luis (B, D).
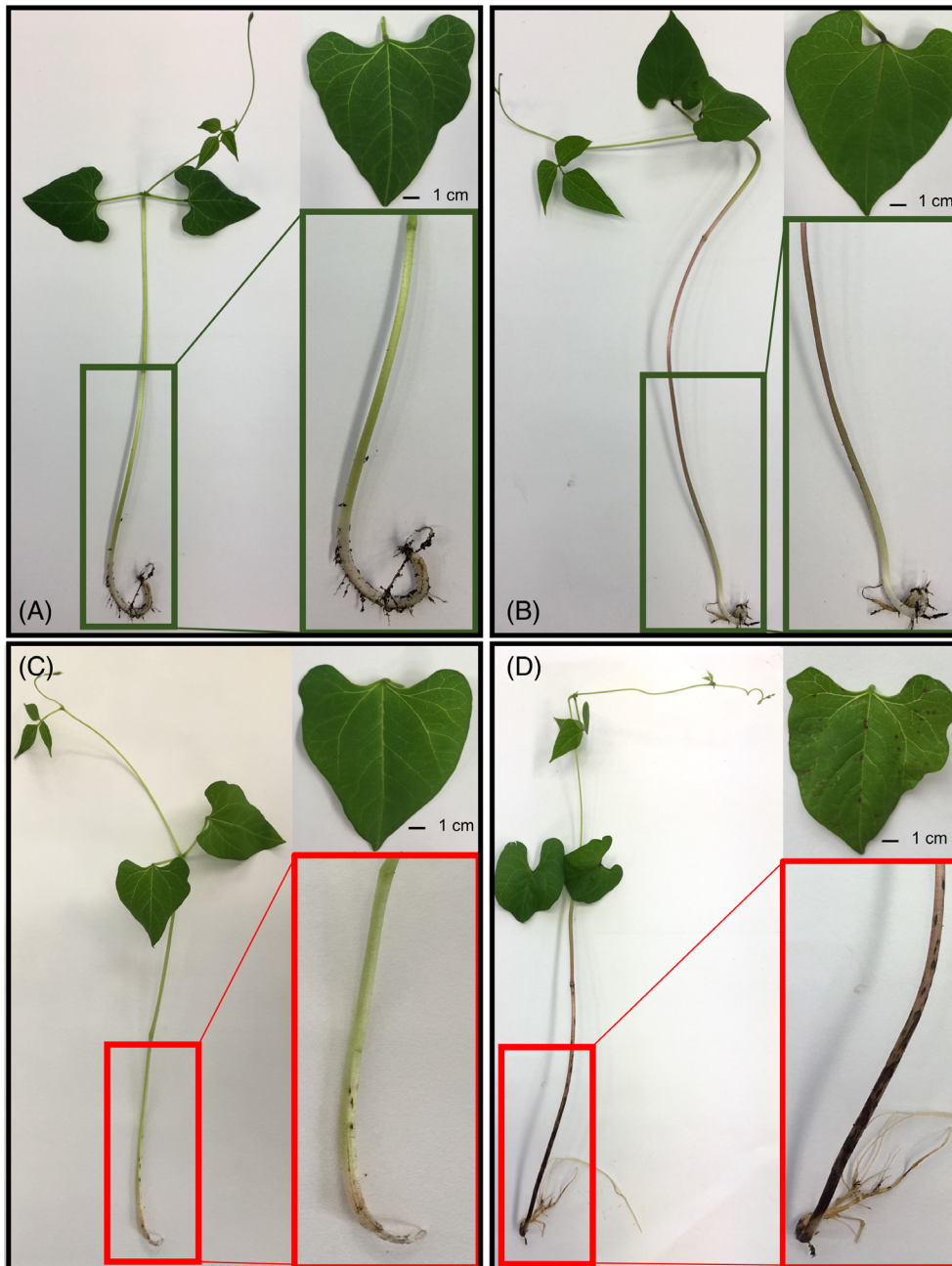
leaves and first true leaves, while no symptoms of the disease were visible on the leaves of R^+ plants (Figure 2).

3.2 | Volatilome analysis

In terms of overall fluxes, R^- plants emitted a significantly higher amount of VOCs (5.13 ppb g^{-1}FW) than R^+ (3.65 ppb g^{-1}FW), while in S^- (3.97 ppb g^{-1}FW) and S^+ (3.98 ppb g^{-1}FW) VOC emission was not different, and similar to R^+ emission. After threshold filtering and blank subtraction, 69 mass peaks were obtained (Dataset S1), on which statistical analysis was performed. These peaks, putatively identified according to available data in literature and/or with genuine standards, were grouped according to structural class (short-chain oxygenated VOCs, fatty acid derived, isoprenoids, benzenoids, sulphides, other VOCs) (Figure S1). The short-chain oxygenated VOCs were the most abundant, driven by high methanol emissions in all conditions. Benzenoids were more abundant in R^- plants compared to other treatments. Fatty acid derivates and isoprenoids were emitted more in R^- than in R^+ plants, but showed an opposite trend in S^- and S^+ plants.

In order to estimate the degree to which the common bean volatilome is determined by genotype and treatment, we applied a PCA,
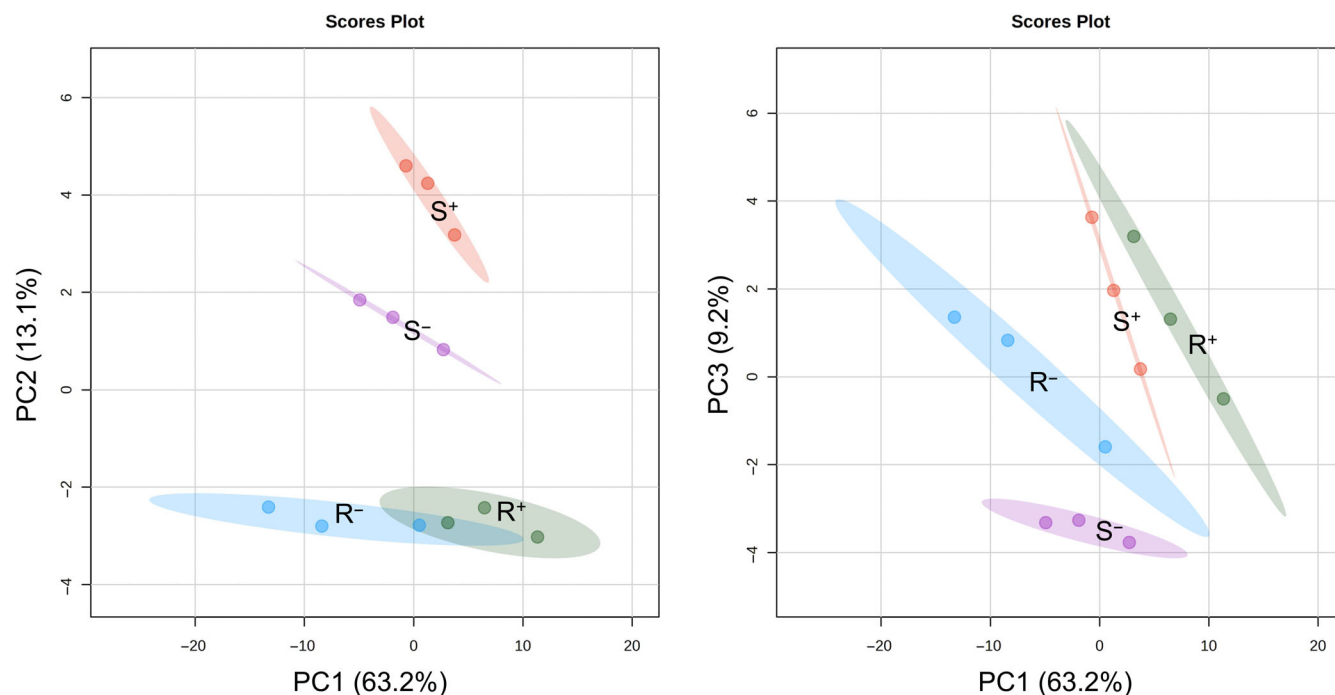
FIGURE 3 Principal component analysis (MetaboAnalyst 5.0) of PTR-QiToF-MS data of volatile organic compound blends. Samples were collected from three biological replicas of moderately resistant controls (R⁻, red), moderately resistant infected plants (R⁺, green), susceptible controls (S⁻, violet) and susceptible infected plants (S⁺, light blue). The percentage of variance explained by each component is reported in brackets.
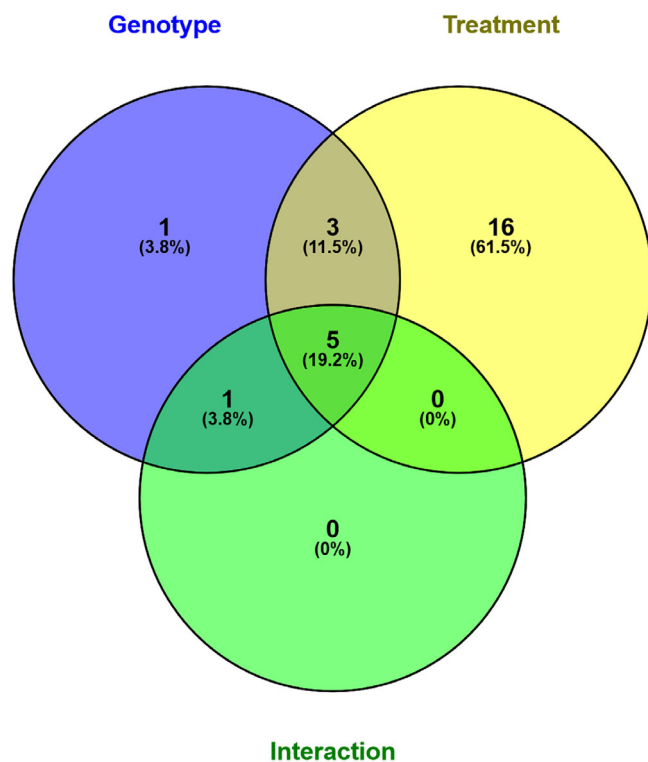

FIGURE 4 Venn diagram (from VENNY 2.1) highlighting the distribution of the identified volatile organic compounds in genotype (G), treatment (*Colletotrichum* infection) (C), or interaction-dependent (I) groups, based on a two-way ANOVA test ($p < 0.05$; MetaboAnalyst 5.0).

which revealed a clear separation of the four conditions and, in particular, a separation of the volatilome emitted from control versus infected S plants (Figure 3). The first three principal components (PC1, PC2, and PC3) explained 85.5% of the total variance (Figure 3A,B). The genotype effect was described by PC2 (13.1% of total variance; Figure 3A), while the PC1 and PC3 described the treatment effect on both genotypes (Figure 3B). A two-way ANOVA identified 10, 24, and 6 VOCs dependent on genotype (G), treatment (*Colletotrichum* infection, C) and interaction (I), respectively (Table S2). The larger number of C-dependent VOCs suggests that the pathogen influences VOCs more than the genotype, while the I factor seems to have a limited additional effect on the volatilome (Figure 4).

The differential effect of genotype and treatment on the abundance of VOCs emitted was displayed as a heatmap (Figure 5), which shows that, among the I-dependent VOCs, hexanal or Z-3-hexen-1-ol (m/z 101,089, $C_6H_{13}O^+$) were released by S⁻ in higher amounts than R⁻ plants. This difference is more evident once the two genotypes were infected with *C. lindemuthianum* since hexanal or Z-3-hexen-1-ol emission increased in S⁺, while largely decreasing in R⁺ plants (Figure 5). Allene or 1,2-propadiene (m/z 41,039, $C_3H_5^+$), also an I-dependent VOC, was emitted only by R-plants.

Among the G-dependent VOCs, 2-cyclopenten-1-one showed a trend similar to hexanal: increasing in S⁺ and disappearing in R⁺ plants.

Finally, among the C-dependent VOCs, ethanol (m/z 47,049, $C_2H_7O^+$) decreased in both bean genotypes when challenged with the pathogen, but this reduction was much more evident in S⁺ plants.
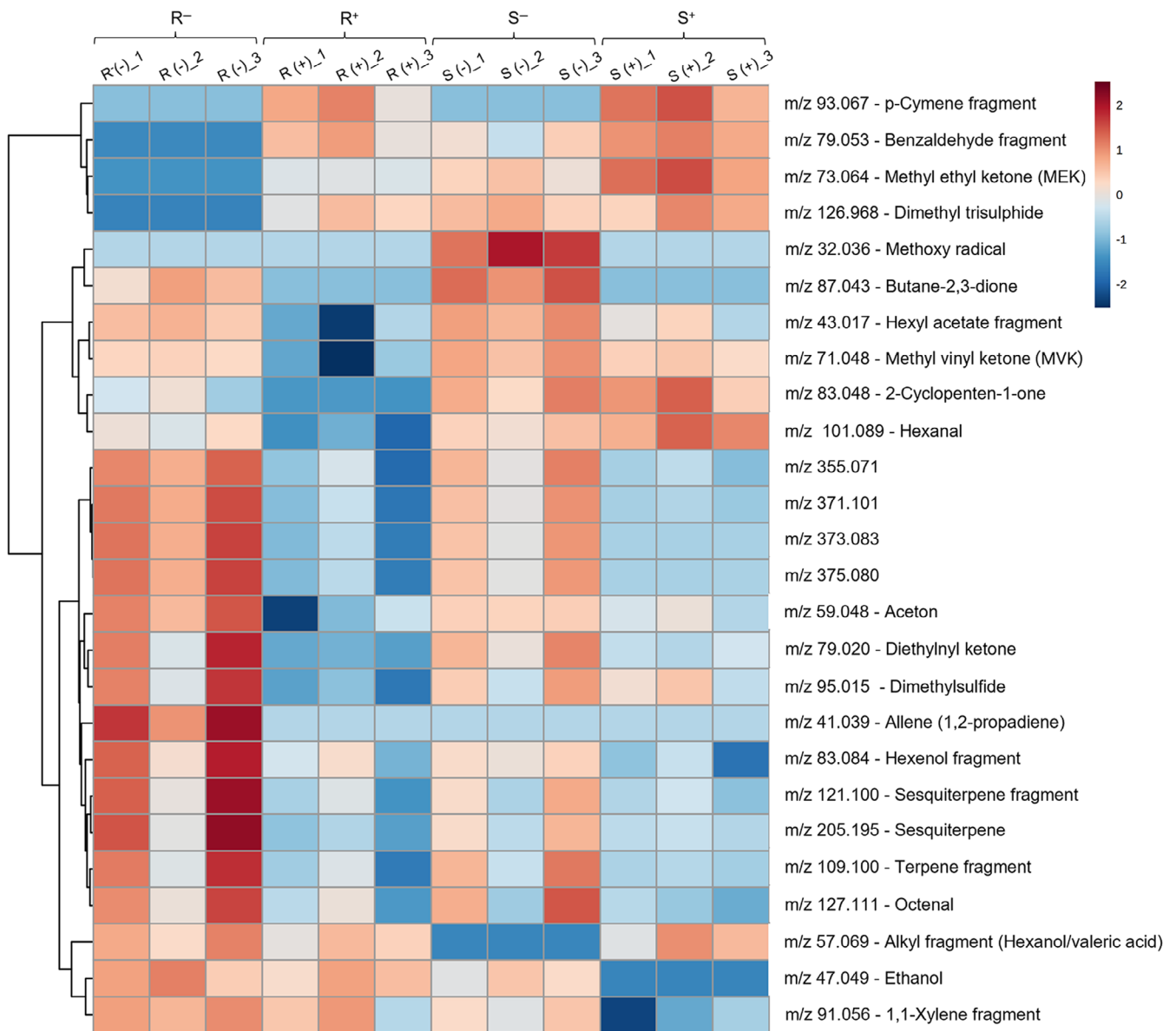
FIGURE 5 Heatmap of significantly abundant volatile organic compounds (VOCs) ($p < 0.05$; MetaboAnalyst 5.0) emitted by moderately resistant (R) and susceptible (S) genotypes in control ($^-$) and infected ($^+$) conditions. VOCs are grouped according to abundance similarity due to both genotype and treatment effects; the abundance of VOCs emitted is described by the colorimetric scale, shading from blue (less abundant VOCs) to red (more abundant VOCs). The list of molecules on the right side is a putative identification according to available data in literature and/or with genuine standards.

Comparing S$^+$ with S$^-$ volatilomes, we found four more-emitted and 13 less-emitted VOCs in S$^+$ plants. Whereas, comparing R$^+$ and R$^-$, we identified four more-emitted and 53 less-emitted VOCs in R$^+$ plants (Figure 5). Three out of the four more-emitted VOCs were common to S$^+$ and R$^+$ plants (2-butanone MEK, m/z 73,064, $C_4H_9O^+$; benzaldehyde, m/z 79,053, $C_6H_7^+$; p-cymene fragment, m/z 93,067, $C_7H_9^+$) while butene (m/z 57,069, $C_4H_9^+$) was more emitted only in S$^+$ versus S$^-$ and dimethyl trisulphide (m/z 126,968, $C_2H_7S_3^+$) was more emitted only in R$^+$ versus R$^-$. Among the less-emitted VOCs, the emission of 2.3-butanedione (m/z 870,434, $C_4H_7O_2^+$) was strongly impaired in both S$^+$ and R$^+$ plants.

3.3 | Gas exchange and stomatal conductance analysis

The stomatal conductance of the leaves is shown in Figure 6. We observed that gH$_2$O values were significantly higher in the susceptible than in the moderately resistant genotype under control conditions (compare R$^-$ and S$^-$). Fungal infection elicited stomatal opening and largely increased stomatal conductance of the sensitive genotype (S$^+$), whereas the stomatal conductance was similar to that observed in control conditions in the moderately resistant genotype (R$^+$).
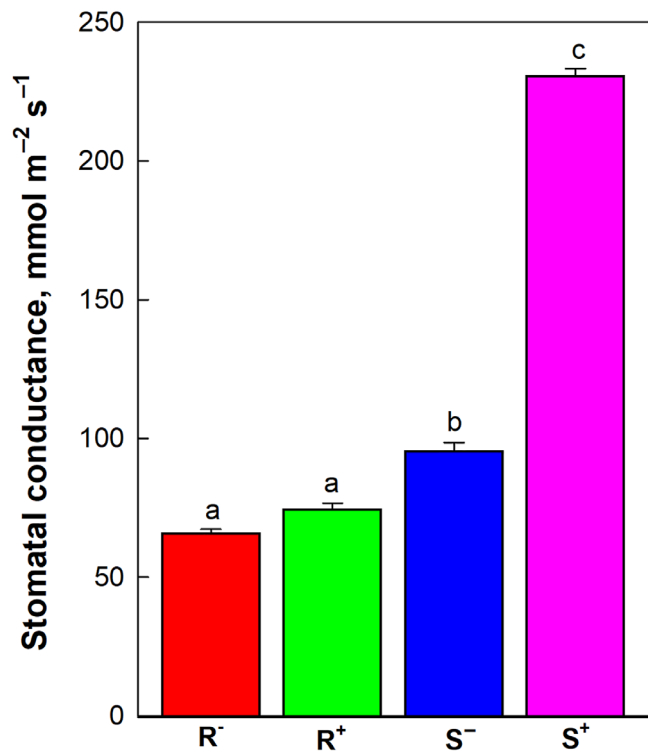
FIGURE 6 Response of stomatal conductance (gH$_2$O) in susceptible (S) and moderately resistant (R) genotypes in control ($^-$) and infected ($^+$) conditions. All data are means ± SE. Different letters indicate statistically significant differences ($p < 0.01$, ANOVA, post-hoc Tukey test).

3.4 | SA and JA precursors analyses

HPLC-MS/MS analyses were performed to monitor the accumulation of defense hormones (SA and JA) and some of their precursors (lipid molecules). SA was significantly more abundant in S$^+$ than in all other treatments (Figure 7A), whereas JA-precursors (especially polyunsaturated fatty acids) were triggered in R$^+$ only (Figure 7E,F).

3.5 | Proteome quality control and overview of quantitative proteomics analysis

Quantitative proteomic analysis using LC-MS/MS was performed to study the molecular differences, at protein level, between moderately resistant and susceptible genotypes after *C. lindemuthianum* infection occurred. The proteomic study identified a total of 2721 proteins assigned to *P. vulgaris* (Dataset S2). The total proteins of the four experimental conditions plotted closely in the PCA (Figure S2); the two genotypes were well-separated on PC2, which accounts for 18.6% of the total variation. PCA also showed a distinct separation between infected and non-infected S plants, as obtained by comparing volatilomes (Figure 3). DAPs obtained from the one-way ANOVA consistency test (FDR < 0.05) and statistically significant in at least

one comparison represented the 9% of the whole protein dataset (250 proteins) (Dataset S3).

3.6 | The *P. vulgaris* proteome genotype-, treatment-, and interaction-dependent differences

A two-factorial ANOVA on the 250 DAPs confirmed a significant genotype effect on 64 proteins (G-DAPs), while the infection treatment had a significant effect on 25 proteins (C-DAPs) and a significant interaction was confirmed for 174 proteins (I-DAPs). I-DAPs (110) were more abundant in S$^+$ than in R$^+$ plants, indicating stronger changes in the proteome of the susceptible genotype after infection (Table S3A–C).

According to the functional classification of DAPs (Figure S3), the 64 G-DAPs were involved in "protein-related" processing (20%), "signaling" and "stress" (6%), "transport" (5%), "cell wall," "RNA" and "amino acid metabolism" (3%), "secondary metabolism" and "hormone metabolism" (1.5%) processes. The 25 C-DAPs were equally distributed among "stress," "RNA," "cell wall," and "amino acid metabolism" categories (8%), with an exception made for "protein-related" group (about 12% for each category). The 174 I-DAPs mostly belonged to the functional classification of "protein-related" processing (12%), "RNA-related" (7%), "cell organization" (6%), "stress" (5%), "signaling" (4%) processes.

3.7 | Identification of hub proteins

Neither G-DAPs nor C-DAPs showed proteins biologically connected. On the contrary, among the I-DAPs, a PPI network containing 172 nodes (proteins) and 113 edges (interactions) was constructed using the STRING online database. The PPI enrichment *p*-value was 0.00794, indicating that I-DAPs are biologically connected (Figure S4). The nine significant interactome members that serve as central hubs were: Imidazole glycerol-phosphate dehydratase (IGPD;V7BCG1), Pyrroline-5-carboxylate reductase (P5CR; V7CV89), Matrin-type domain-containing protein (V7BXY; AT2G32600), DNA-directed RNA polymerase subunit (NRPB1; V7CLS7), DUF1716 domain-containing protein (V7BPH9; AT3G02710), Aspartokinase (AK-LYS1; V7C2X5), Ribosomal_S13_N domain-containing protein (V7CE67), RNA helicase (V7CGX3), RRM domain-containing protein (U1-70K; V7CI13).

4 | DISCUSSION

When challenged with *C. lindemuthianum*, the two bean genotypes exhibited very different behaviors. As expected, the susceptible genotype showed more severe symptoms, with diffuse necrosis on stems and leaves. We analyzed the responses of the volatilome and proteome of the two genotypes, especially aiming at identifying changes that may be important in terms of resistance to the pathogen infection.
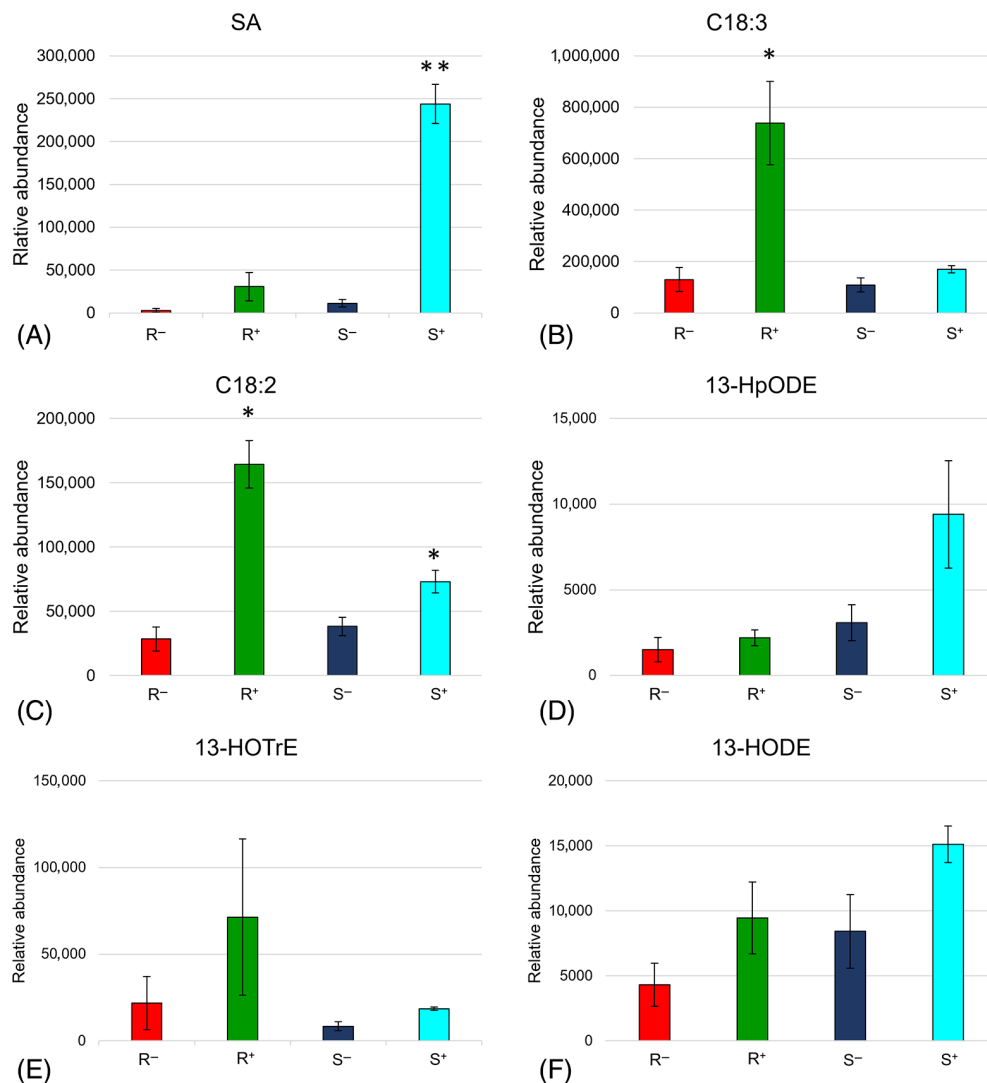
Physiologia Plantarum

FIGURE 7 HPLC-MS-MS measurements of (A) salicylic acid (SA), (B) linolenic acid (C18:3), (C) linoleic acid (C18:2), (D) 13-hydroperoxy-9,11-octadecadienoic acid (13-HpODE), (E) 13-hydroxy-9,11,15-octadecatrienoic acid (13-HOTrE), (F) 13-hydroxyoctadecadienoic acid (13-HODE). Measurements were carried out in susceptible (S) and moderately resistant (R) genotypes in control ($^-$) and infected ($^+$) conditions. Bars represent the means ± standard error of three biological replicates technically repeated two times. Asterisks above the bars indicate significant differences between the ($^-$) and ($^+$) treatments (Two-way ANOVA, based on multiple-sample tests FDR adjusted value $*p < 0.05$; $**p < 0.01$).

4.1 | *C. lindemuthianum* induces the emission of few VOCs, mainly in susceptible beans

The PCA of the volatilomes of two bean genotypes, infected and non-infected, was clearly able to discriminate among the conditions; the volatilomes of S$^+$ and R$^+$ plotted much closer than those of S$^-$ and R$^-$ (Figure 3B), demonstrating an existing genotype-based difference between R$^-$ and S$^-$ volatile emissions.

Proteomic results highlight the presence, into the I-DAPs list, of two proteins playing fundamental roles in stomatal opening. Munc-13-like protein (AT5G06970.1) and phototropin 1 (AT3G45780.1) (Hashimoto-Sugimoto et al., 2013; Takemiya et al., 2013) accumulated more in S$^+$ than in R$^+$ plants. This result was corroborated by the stomatal conductance experiment, which showed a higher gH$_2$O in S$^+$ plants compared to all other treatments. Similar results were obtained by Prats et al. (2006), who showed an impaired stomatal opening on the pathosystem barley-*Blumeria graminis* by using barley mutants responding with a strong HR when challenged with the biotrophic fungal pathogen. Also, Rippa et al. (2023) reported a four times higher stomatal conductance in *Botrytis cinerea* infected pepper tissues compared to controls.

Furthermore, none of the VOCs was exclusively elicited in R$^+$ plants, which suggests no association between resistance to *C. lindemuthianum* infection and VOC emission. However, the following observations can also be made when comparing volatilome and proteome of the two bean genotypes.

Among the C-dependent VOCs, emission of the monoterpene p-cymene (retrieved as a fragment m/z 93,067, $C_7H_9^+$ that usually represents 70%–100% of the molecular ion; Malekenia et al., 2007) was stimulated in both genotypes when infected by *C. lindemuthianum*. p-Cymene is a constituent of essential oils, characterizing the scent of many aromatic plants, such as cumin, oregano, and thyme. When accumulated in specialized plant structures, p-cymene is known for its antibacterial, antiviral, and antifungal activities (Singh & Pandey, 2021) and its stimulation in both infected genotypes (Figure 8A) indicates the activation of the metabolic pathway producing monoterpenes (the MEP pathway; Lichtenthaler, 1999) induced by the pathogen infection. De novo synthesis of isoprenoids in response to pathogen infection has been reported in numerous plants. For example, isoprenoids are induced in poplars susceptible to the rust fungus *Melampsora*
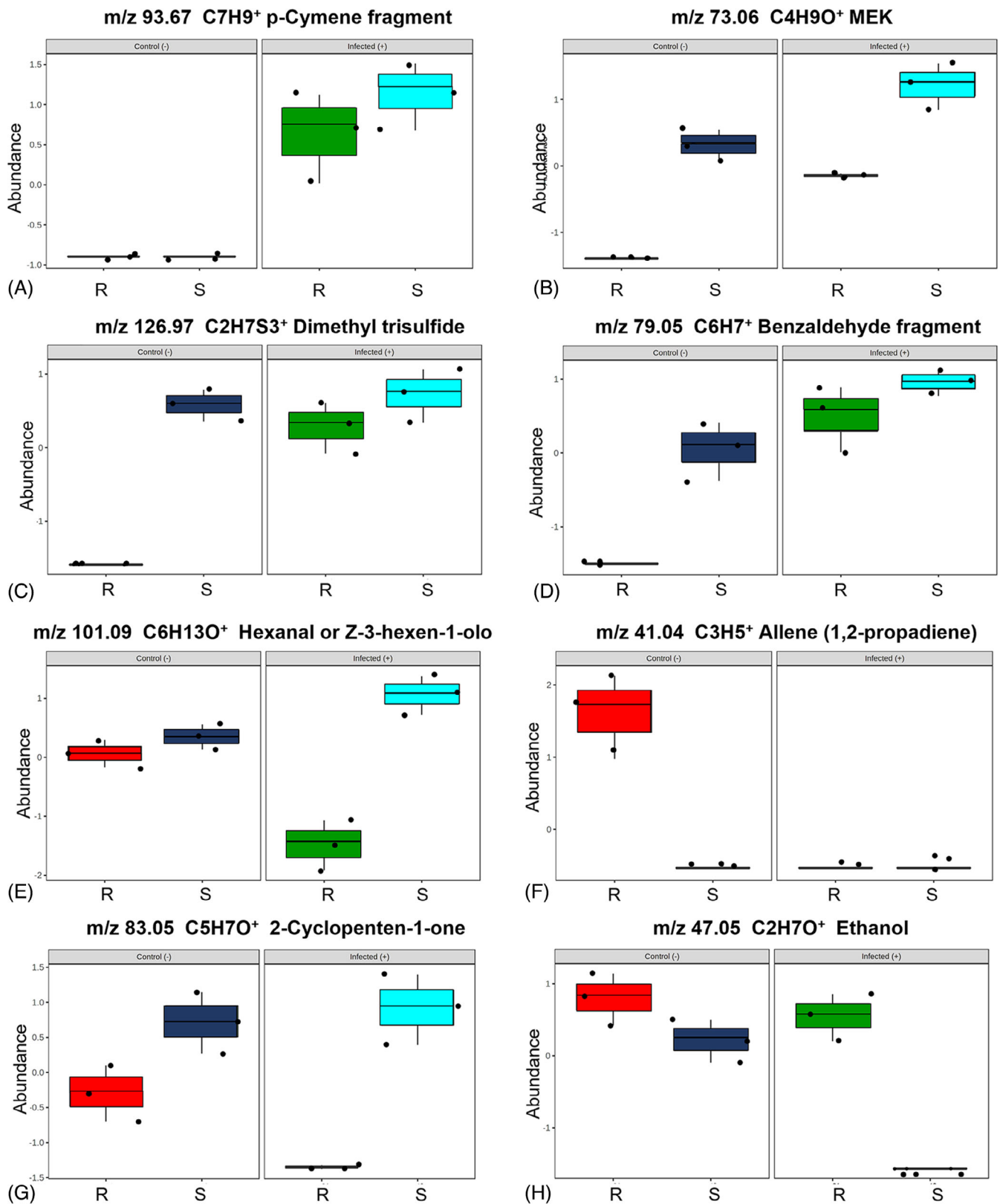
FIGURE 8 Graphical representation of abundance of some statistically significant volatile organic compounds, identified by two-way ANOVA, emitted by moderately resistant (R) and susceptible (S) genotypes in control ($^-$) (colored in red and blue, respectively) and infected ($^+$) (colored in green and light blue, respectively) conditions. (A) p-cymene, (B) methyl-ethyl-ketone (MEK), (C) dimethyl trisulphide, (D) benzaldehyde fragment, (E) hexanal or Z-3 hexen-1-ol, (F) allene (1,2-propadiene), (G) 2-cyclopenten-1-one, and (H) ethanol (FDR adjusted value $p < 0.05$). Abundance values refer to Log_{10}-transformed and auto-scaled ppb g^{-1}fw values (MetaboAnalyst 5.0).

laricipopulina (Eberl et al., 2018). To the best of our knowledge, this is the first time that p-cymene is detected as a Pathogen-Induced Plant Volatile (PIPV) in *P. vulgaris* volatilome, but we do not know whether, at the detected dose, this VOC is able to exert any anti-fungal activity in beans. In fact, other monoterpenes that are generally co-synthesized by the same pathway were not statistically differentially emitted, suggesting a specific role of p-cymene in this plant-pathogen interaction.

Methyl ethyl ketone (m/z 73,064 C_4H_8O; MEK, also known as 2-butanone, butanone, methyl acetone, butan-2-one, methyl propanone and ethyl methyl ketone) is an oxygenated volatile organic compound produced by plants (Bracho-Nunez et al., 2013; Brilli et al., 2014), fungi (Wheatley et al., 1997), and bacteria (Song & Ryu, 2013; Wilkins, 1996). Yáñez-Serrano et al. (2016), conducting an extensive field measurement, demonstrated that MEK is emitted by vegetation and also by other biogenic sources, like dead and decaying plant matter. Biosynthetic pathways for MEK production in plants are not completely elucidated. Fall (2003) suggested that MEK is a bioproduct of a cyanohydrin lyase reaction during cyanogenesis, but MEK is also emitted in non-cyanogenic species (Yáñez-Serrano et al., 2016). Cappellin et al. (2019) showed that MEK can be made by in planta transformation of methyl vinyl ketone, a bioproduct of isoprene. In our analysis, isoprene was not emitted at statistically different rate, and MEK was G- and C-dependent, and stimulated in both infected genotypes (Figure 8B). We are not sure about of the significance of MEK emission and cannot exclude that MEK could be also produced by the pathogen during its necrotrophic growth.

Similar to MEK, two G-dependent VOCs corresponding to m/z 126,968 and m/z 79,053 were also constitutively emitted by S^- plants but not by R^- plants. *C. lindemuthianum* infection clearly further elicited the emission of these two VOCs both in S and R plants (Figure 8C,D). Putatively, the m/z 126,968 peak could correspond to dimethyl trisulphide (Figure 8C). Sulfur-containing VOCs, as glucosinolates and/or their breakdown products, are known for their fungicidal, bactericidal, nematocidal, and allelopathic properties (Fahey et al., 2001), but glucosinolate production has not been reported in *Phaseolus vulgaris*, although our proteomic analysis supports the idea that glucosinolate production is elicited in infected beans. *C. lindemuthianum* infection induced accumulation of tryptophan synthase beta type 2 (V7BZU9) (see C-DAPs list; Table S3B), an enzyme producing tryptophan, a precursor of secondary metabolites as camalexin and glucosinolates (Barth & Jander, 2006; Bednarek et al., 2009).

A peak corresponding to m/z 79,053 was putatively identified as a fragment of benzaldehyde, which was more emitted in both infected genotypes (Figure 8D). Benzaldehyde can be produced through the shikimic pathway (shared with phenylpropanoids and SA). Two core phenylpropanoid pathway enzymes in the I-list, cinnamate 4-hydroxylase (AT2G30490.1) and chorismate mutase (V7CUM8), showed differential accumulation before and after fungal infection. The proteome and volatilome results were supported by the presence of SA in the leaves of S^+ plants compared to the other samples (Figure 7A). Higher emission of benzaldehyde by S^+

plants could indicate a shift of the metabolic pathways toward the production of SA confirmed by direct measurements of a high amount of SA in S^+, while benzaldehyde could be directed toward different metabolic pathways in R^+ plants.

Hexanal is part of the important group of plant GLVs. These six carbons (C6) compounds, including alcohols, aldehydes, and esters (Dudareva et al., 2006), are generated through the oxylipin pathway from C18-polyunsaturated fatty acids (α-linolenic acid and linoleic acid) by membrane lipids hydrolysis (Matsui et al., 2006). Green Leaf Volatiles (GLVs) are usually synthesized and emitted by leaves exposed to abiotic stresses (Brilli et al., 2011). However, they are also produced after fungal infection and seem to act as aerial messengers to prime neighboring plants (Ul Hassan et al., 2015). Ameye et al. (2018) showed enhanced GLV emission in response to fungal treatments, wounding, and herbivory. In maize, GLVs were recently shown to be related to susceptibility to *Colletorichum graminicola* (Gorman et al., 2020). Perhaps GLVs are a marker of cellular oxidative damage, particularly evident in necrotrophic fungi infections. Furthermore, in our study, the emission of hexanal was stimulated by the pathogen in the susceptible genotype, whereas GLVs were significantly less emitted in R^+ plants compared to all other treatments (Figure 8E). We can hypothesize a different genotypic response to the pathogen leading to GLV release (Ameye et al., 2018; Verhage et al., 2010) (see below, proteomic discussion).

The oxylipin pathway is also involved in JA production, an important defensive hormone (Castillo et al., 2004; Pinfield-Wells et al., 2005; Schilmiller et al., 2007). We have identified at least two VOCs produced in this same pathway: allene or 1,2-propadiene (m/z 41,039, $C_3H_5^+$) and 2-cyclopenten-1-one (m/z 83,048, $C_5H_7O^+$) (Figure 8F,G). Both VOCs were suppressed in R^+ plants, confirming a general down-regulation of the oxylipin pathway in the moderately resistant genotype after infection. We speculate that these VOCs were less emitted after infection due to a different allocation of intermediates or by-products of oxylipin pathway. In fact, in R^+ plants, the allene oxide cyclase (AOC) was more accumulated and, consequently, allene disappeared.

2-Cyclopenten-1-one, besides being a by-product of the oxylipin pathway, can be involved in plant protection as demonstrated by (Kourtchenko et al., 2007): the Arabidopsis mutant (*opr3*), defective in the isoform of 12-oxo-phytodienoate (OPDA) reductase required for JA biosynthesis but still producing 2-cyclopenten-1-one, is resistant to the necrotrophic pathogen *Alternaria brassiciola* and to the insect *Bradysia impatiens*.

Stress-induced changes of VOC blend were mirrored at proteomic level. Among the I-DAPs, LOX protein (V7ASA9), peroxisomal 3-ketoacyl-CoA thiolase 3 (AT2G33150.1) and RNA helicase (V7CGX3) accumulated in S^+ plants. It should be observed that the latter is a hub protein (Figure S4) involved in JA-mediated signaling pathways. Interestingly, RNA helicase Arabidopsis mutants showed altered levels of LOX2 (Sakr et al., 2018; Shi et al., 2012).

Plant defense against pathogenic agents usually operates through a complex network of "defense hormones" such as SA, JA, and ethylene (ET). Their relative fine-tuning switches on/off appropriate

responses to pathogens with different lifestyle. Typically, the SA signaling pathway is active if the plant is challenged by a biotrophic pathogen, whereas the JA/ET signaling pathway takes over in the presence of necrotrophic pathogens. Nevertheless, a "contamination" among these pathways may occur (Robert-Seilaniantz et al., 2011). Moreover, pathogens can overcome plant defenses by manipulating these pathways. In another pathosystem involving a species belonging to *Colletotrichum* genus (namely, *Fragaria × ananassa* Duch. and *Colletotrichum acutatum*), SA and JA pathways were impaired, resulting in some advantages for fungal spreading (Amil-Ruiz et al., 2016). In our system, SA was elicited in S^+, whereas JA precursors (especially polyunsaturated fatty acids) were triggered in R^+. We might speculate that the pathogen manipulates the SA response in S^+ plants. By inducing cell death, the pathogen expedites its necrotrophic growth in S plants, while the moderately resistant genotype succeeds to limit pathogen contamination by enhancing the JA pathway. We did not find JA or its active conjugate jasmonoyl isoleucine (JA-Ile) in S^+ as well as in R^+, but their precursors were (significantly in case of polyunsaturated fatty acids) more abundant in R^+ plants. We can suggest that, even if the R^+ plants are moderately resistant to the pathogen, *C. lindemuthianum* succeeds in harnessing JA "maturation" and JA-related pathways, thus limiting plant defenses. Indeed, the enzymes (AOS and AOC) accumulated more in R^+ than in S^+ (Table S3).

Among short-chain oxygenated VOCs, ethanol emission pattern also deserves to be highlighted. Ethanol was constitutively emitted by S^- and R^- plants, but its emission only dropped in the susceptible plants after *C. lindemuthianum* infection (Figure 8H). Ethanol is generally produced by anaerobic fermentations of plants (cotyledonal leaves, stems, flowers, or even necrotic tissues) under hypoxia or anoxia conditions (Ventura et al., 2020). In our experiments, the reduced emission of ethanol in S^+ plants could reveal a more aerobic condition inside the leaves due to high stomatal conductance (Figure 6).

4.2 | Proteomic analysis provides a general molecular framework of genotypic differences and defense mechanisms activated by the pathogen

Among C-DAPs that accumulated after *C. lindemuthianum* infection in both genotypes, we identified several proteins that could be involved in plant defense response. Among them, phosphatase 2A regulatory subunit TAP46 (V7AWB1) plays multifaceted roles in biotic stress perception, signaling and response, and in plant immunity. DEAD-box ATP-dependent RNA helicase 37 (V7BIK6) is involved in mRNA quality control, fine-tuning transcript levels to reduce fitness costs and achieve effective immunity (Jung et al., 2020; Sulkowska et al., 2020); arginosuccinate synthase (V7CBE7) is involved in the synthesis of L-arginine, an important amino acid for nitrogen storage and to fine-tune the production of NO (Winter et al., 2015). In *A. thaliana*, a reduction in arginine levels promotes the growth of *Pseudomonas syringae* (Anwar et al., 2019). On the contrary, the abundance of

dihydrofolate reductase (V7CUJ1) and basic endochitinase B (V7CG25) were strongly decreased in both genotypes. Dihydrofolate reductase regulates the folate pathway, which participates in fine-tuning NADPH production, cellular reducing power, and ROS levels (Gorelova et al., 2017). In *A. thaliana*, the disruption of the folate pathway has been shown to enhance the resistance against *Pseudomonas syringae* pv. *tomato* DC3000 via the activation of a primed immune state, whereas the stimulation of folate results in an enhanced susceptibility (González & Vera, 2019). Basic endochitinase B is involved in ET- and JA-mediated signaling pathways during the SAR. The *Capsicum annuum* homolog of basic endochitinase B (CaChiIII7) is transcriptionally stimulated by *C. acutatum* infection. Knockdown of *CaChiIII7* reduced the expression of several defense response-related genes in pepper leaves upon *C. acutatum* infection, whereas the transient expression of *CaChiIII7* increased their expression, resulting in the induction of a hypersensitive response (HR) and biosynthesis of hydrogen peroxide (Ali et al., 2020).

The picture emerging from the analysis of the I-DAPs is more complex and informative. In particular, cell wall stability, the first line of defense against *C. lindemuthianum*, seems to explain the better resistance to this pathogen colonization in R than in S genotype. Not only, as previously discussed, proteomic results show an alteration of the proteins involved in stomatal opening, but also R^+ accumulated several proteins specifically involved in cell wall reinforcement and protein delivery to the plasma membrane. These included proteins associated with cell wall tensile strength and integrity (e.g., Syntaxin/t-SNARE family protein [V7CWZ1], Novel Plant Snare 13 [V7C8E7], and the Trichome Birefringence-Like 39 protein [AT2G42570.1]), extracellular medium alkalization and accumulation of phenolic compounds (e.g., flavin mononucleotide hydrolase 1 [V7B1G5] and farnesyltransferase A [V7BWN0]) (Boubakri et al., 2013; Escamilla-Treviño et al., 2006; Gille & Pauly, 2012; Hochholdinger et al., 2008; Jalakas et al., 2017; Liu et al., 2010; Taheri & Tarighi, 2011; Zhang et al., 2009). It should be observed that differences in cell wall composition characterize R and S genotypes. Indeed, in the G-DAPs list, several enzymes involved in the biosynthesis of cuticular wax and cutin (AMP-dependent synthetase and ligase family protein, V7BJB3), hemicellulose (Cellulose Synthase-like E1, V7B9B7), xyloglucan (Glycosyl Hydrolase family protein, V7B6Y9), and alpha/beta-hydrolase superfamily protein (V7BLY4), accumulated more in R than in S.

Notably, the level of MLO protein (V7BGV6), a negative regulator of plant defense (Acevedo-Garcia et al., 2014; Zheng et al., 2013), was also lower in R^+ than in S^+ plants in the I-list. In the same list, Aspartokinase (V7C2X5) accumulated in R^- more than in S^- and to levels comparable with S^+ and R^+. Aspartokinase is a hub protein, crucial in the Asp-derived amino acid pathway: regulation of Asp content, fluxes and transport has recently been recognized as critical for plants to counteract biotic stresses (Han et al., 2021).

Based on these observations, it seems reasonable to assume that the R genotype displays a stronger first line of defense against *C. lindemuthianum*, which is crucial to control disease progression. On the contrary, *C. lindemuthianum* infection proceeds more rapidly in the
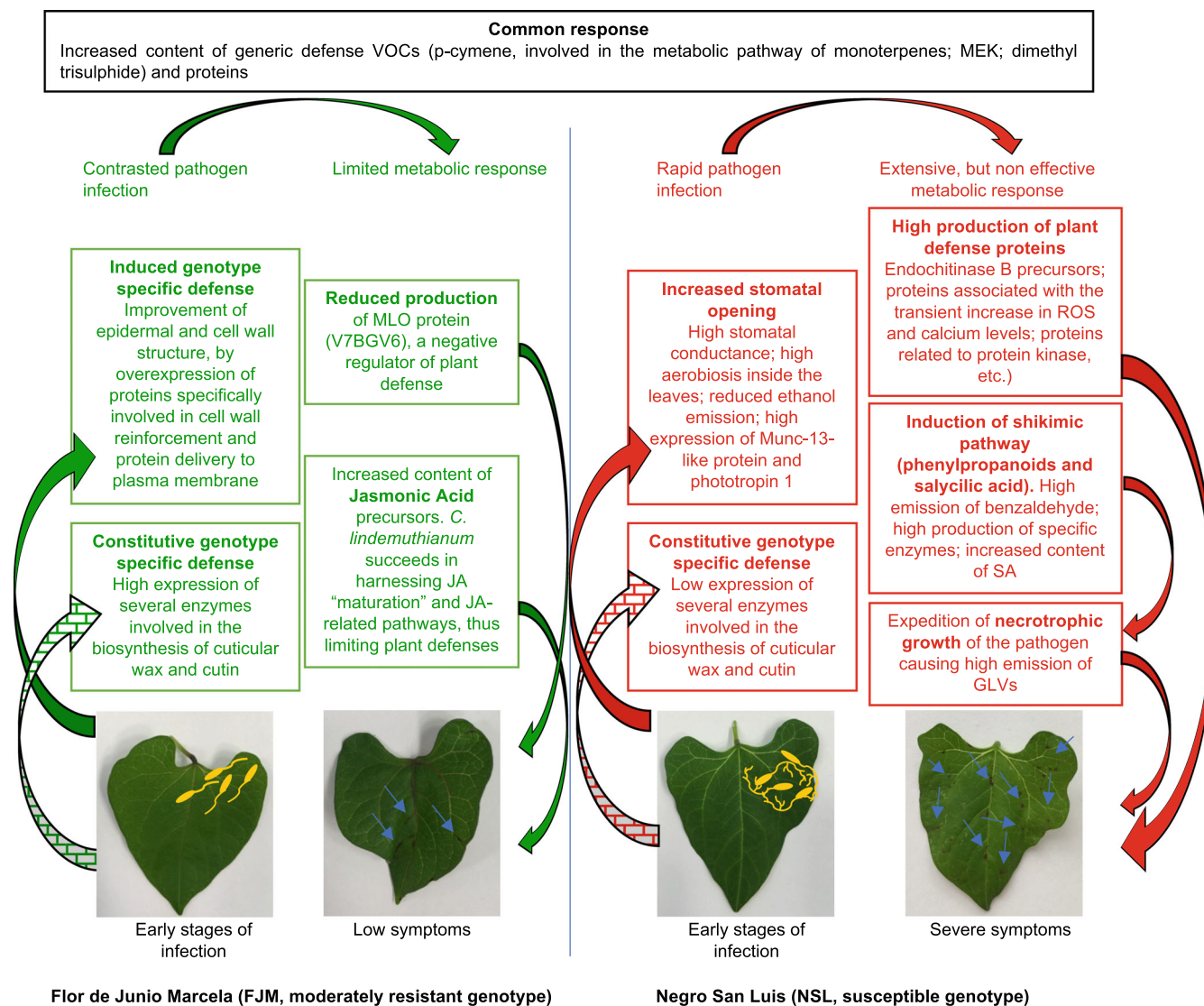
Common response
Increased content of generic defense VOCs (p-cymene, involved in the metabolic pathway of monoterpenes; MEK; dimethyl trisulphide) and proteins

Contrasted pathogen infection — Limited metabolic response

Rapid pathogen infection — Extensive, but non effective metabolic response

Induced genotype specific defense
Improvement of epidermal and cell wall structure, by overexpression of proteins specifically involved in cell wall reinforcement and protein delivery to plasma membrane

Reduced production of MLO protein (V7BGV6), a negative regulator of plant defense

Increased content of **Jasmonic Acid** precursors. *C. lindemuthianum* succeeds in harnessing JA "maturation" and JA-related pathways, thus limiting plant defenses

Constitutive genotype specific defense
High expression of several enzymes involved in the biosynthesis of cuticular wax and cutin

Increased stomatal opening
High stomatal conductance; high aerobiosis inside the leaves; reduced ethanol emission; high expression of Munc-13-like protein and phototropin 1

Constitutive genotype specific defense
Low expression of several enzymes involved in the biosynthesis of cuticular wax and cutin

High production of plant defense proteins
Endochitinase B precursors; proteins associated with the transient increase in ROS and calcium levels; proteins related to protein kinase, etc.)

Induction of shikimic pathway (phenylpropanoids and salicilic acid). High emission of benzaldehyde; high production of specific enzymes; increased content of SA

Expedition of **necrotrophic growth** of the pathogen causing high emission of GLVs

Early stages of infection — Low symptoms

Early stages of infection — Severe symptoms

Flor de Junio Marcela (FJM, moderately resistant genotype)

Negro San Luis (NSL, susceptible genotype)

FIGURE 9 Schematic representation of the model proposed for the response of the two bean genotypes with different susceptibility to *Colletotrichum lindemuthianum* infection.

S genotype, leading to a more extensive metabolic response against fungal attack. Consistently, many I-DAPs related to plant defense induction upon pathogen infection were less abundant in R$^+$ than in S$^+$ plants. This list includes: two basic endochitinase B precursors (V7CH45, V7AUH2); proteins associated with the transient increase in ROS and calcium levels (MLP-like protein 43, V7AIR2; Calcium-binding EF-hand family protein, V7BXX6); proteins related to protein kinase activation (Mitogen-activated protein kinase kinase 4, V7ATB0), proteolysis (LON1, V7BJ03; FTSH10, V7AFJ9; peptide-N(4)-(N-acetyl-beta-glucosaminyl) asparagine amidase, V7BQ67), endomembrane trafficking and proteasome-dependent processes (Golgin candidate 6, V7C0K5; Vacuolar protein sorting-associated protein 29, V7B6Z5; Vacuolar Sorting Receptor 6, V7B317; RabD1, V7BRE6; Sec5, V7BGR8), secondary metabolite processing (UDP-glycosyltransferase 76F1, V7CZ85) (Fujisaki & Ishikawa, 2008; Koo et al., 2006; Ren et al., 2002; Wang et al., 2016).

Also, levels of Pyrroline-5-carboxylate (P5C) reductase (V7CV89) and three core enzymes of the phenylpropanoid pathway, which

generates a large array of key mediators involved in plant-pathogen interactions (NADPH-cytochrome P450 reductase 1 [V7AVR7], Cinnamate 4-hydroxylase [AT2G30490.1], and Chorismate mutase [V7CUM8]), were more abundant in S$^+$ than in R$^+$ plants. P5C catalyzes the final step in proline biosynthesis and was categorized as hub protein (Figure S4).

5 | CONCLUSIONS

Overall, our volatilome and proteome analyses suggest that two different strategies were activated by the two bean genotypes characterized by different levels of susceptibility/resistance (Figure 9). The moderately resistant genotype (R) probably reduced pathogen infection, invasion and replication investing on a very highly structured epidermis and cell wall. These results agree with previous experimental evidence indicating the containment of *C. lindemuthianum* infection by

the activation of cell wall reinforcement-related genes in resistant plants (Padder et al., 2016). The susceptible genotype (S) failed to reduce pathogen invasion at cell wall level and activated a wider range of defensive biochemical responses, including those involved in the release of VOC markers. The S plants also induced quicker attainment of the fungal necrotrophic phase by the induction of a HR involving the synthesis of GLV and SA together with a loss of stomatal control (Prats et al., 2006). The volatilome of bean plants seems to be more useful as a marker of biochemical changes without being directly involved in defensive responses. It might also play a major role in priming neighboring plants, as already suggested (Quintana-Rodriguez et al., 2015). We believe that this study on the *Colletotrichum*-bean interaction at 21 DAS could serve as a basis for future investigations to shed light on responses during the early stages of infection (biotrophic phase), which were not the focus of the present work.

AUTHOR CONTRIBUTIONS

Michelina Ruocco, Maurilia M. Monti, Marcella Bracale, and Francesco Loreto conceived and contributed to the experimental design; Ilaria Mancini, Marzia Beccaccioli, Rosanna Bossa, Guido Domingo, and Liberata Gualtieri performed the experiments and all authors analyzed and interpreted the data; Michelina Ruocco, Maurilia M. Monti, and Marcella Bracale wrote the original draft and all authors contributed to review and editing. All authors agree with the published version of the manuscript.

ACKNOWLEDGMENTS

CONFLICT OF INTEREST STATEMENT

The authors declare no conflicts of interest.

DATA AVAILABILITY STATEMENT

All data supporting the findings of this study are available within the paper and within its supplementary information published online.

ORCID

Maurilia M. Monti https://orcid.org/0000-0003-4508-7106
Guido Domingo https://orcid.org/0000-0002-2617-8873

REFERENCES

Acevedo-Garcia, J., Kusch, S. & Panstruga, R. (2014) Magical mystery tour: MLO proteins in plant immunity and beyond. *New Phytologist*, 204(2), 273–281.

Albert, I., Hua, C., Nürnberger, T., Pruitt, R.N. & Zhang, L. (2020) Surface sensor systems in plant immunity. *Plant Physiology*, 182(4), 1582–1596.

Ali, M., Li, Q.-H., Zou, T., Wei, A.-M., Gombojab, G., Lu, G. et al. (2020) Chitinase gene positively regulates hypersensitive and defense responses of pepper to *Colletotrichum acutatum* infection. *International Journal of Molecular Sciences*, 21(18), 6624.

Ameye, M., Allmann, S., Verwaeren, J., Smagghe, G., Haesaert, G., Schuurink, R.C. et al. (2018) Green leaf volatile production by plants: a meta-analysis. *New Phytologist*, 220(3), 666–683.

Amil-Ruiz, F., Garrido-Gala, J., Gadea, J., Blanco-Portales, R., Muñoz-Mérida, A., Trelles, O. et al. (2016) Partial activation of SA-and JA-defensive pathways in strawberry upon *Colletotrichum acutatum* interaction. *Frontiers in Plant Science*, 7, 1036.

Anwar, S., Ali, M.A., Abbas, A. & Wieczorek, K. (2019) Arabidopsis Argininosuccinate Lyase and Argininosuccinate Synthase are important for resistance against *Pseudomonas syringae*. *Advancements in Life Sciences*, 7(1), 20–26.

Baldassarre, V., Cabassi, G., Spadafora, N.D., Aprile, A., Müller, C.T., Rogers, H.J. et al. (2015) Wounding tomato fruit elicits ripening-stage specific changes in gene expression and production of volatile compounds. *Journal of Experimental Botany*, 66(5), 1511–1526.

Bardas, G.A., Lagopodi, A.L., Kadoglidou, K. & Tzavella-Klonari, K. (2009) Biological control of three *Colletotrichum lindemuthianum* races using *Pseudomonas chlororaphis* PCL1391 and *Pseudomonas fluorescens* WCS365. *Biological Control*, 49(2), 139–145.

Barth, C. & Jander, G. (2006) Arabidopsis myrosinases TGG1 and TGG2 have redundant function in glucosinolate breakdown and insect defense. *The Plant Journal*, 46(4), 549–562.

Beccaccioli, M., Salustri, M., Scala, V., Ludovici, M., Cacciotti, A., D'Angeli, S. et al. (2021) The effect of fusarium verticillioides fumonisins on fatty acids, sphingolipids, and oxylipins in maize germlings. *International Journal of Molecular Sciences*, 22(5), 2435.

Bednarek, P., Piślewska-Bednarek, M., Svatoš, A., Schneider, B., Doubský, J., Mansurova, M. et al. (2009) A glucosinolate metabolism pathway in living plant cells mediates broad-spectrum antifungal defense. *Science*, 323(5910), 101–106.

Bigirimana, J. & Höfte, M. (2002) Induction of systemic resistance to *Colletotrichum lindemuthianum* in bean by a benzothiadiazole derivative and rhizobacteria. *Phytoparasitica*, 30(2), 159–168.

Boller, T. & Felix, G. (2009) A renaissance of elicitors: perception of microbe-associated molecular patterns and danger signals by pattern-recognition receptors. *Annual Review of Plant Biology*, 60(1), 379–406.

Borges, L., Santana, F., Castro, I., Arruda, K., Ramos, H. & Barros, E. (2015) Two-dimensional electrophoresis-based proteomic analysis of *Phaseolus vulgaris* in response to *Colletotrichum lindemuthianum*. *Journal of Plant Pathology*, 97(2), 249–257.

Boubakri, H., Poutaraud, A., Wahab, M.A., Clayeux, C., Baltenweck-Guyot, R., Steyer, D. et al. (2013) Thiamine modulates metabolism of the phenylpropanoid pathway leading to enhanced resistance to *Plasmopara viticola* in grapevine. *BMC Plant Biology*, 13(1), 1–15.

Bracho-Nunez, A., Knothe, N., Welter, S., Staudt, M., Costa, W.R., Liberato, M.A.R. et al. (2013) Leaf level emissions of volatile organic compounds (VOC) from some Amazonian and Mediterranean plants. *Biogeosciences*, 10(9), 5855–5873.

Bricchi, I., Leitner, M., Foti, M., Mithöfer, A., Boland, W. & Maffei, M.E. (2010) Robotic mechanical wounding (MecWorm) versus herbivore-induced responses: early signaling and volatile emission in Lima bean (Phaseolus lunatus L.). *Planta*, 232(3), 719–729.

Brilli, F., Gioli, B., Zona, D., Pallozzi, E., Zenone, T., Fratini, G. et al. (2014) Simultaneous leaf-and ecosystem-level fluxes of volatile organic compounds from a poplar-based SRC plantation. *Agricultural and Forest Meteorology*, 187, 22–35.

Brilli, F., Loreto, F. & Baccelli, I. (2019) Exploiting plant volatile organic compounds (VOCs) in agriculture to improve sustainable defense strategies and productivity of crops. *Frontiers in Plant Science*, 10, 264.

Brilli, F., Ruuskanen, T.M., Schnitzhofer, R., Müller, M., Breitenlechner, M., Bittner, V. et al. (2011) Detection of plant volatiles after leaf wounding and darkening by proton transfer reaction "time-of-flight" mass spectrometry (PTR-TOF). *PLoS One*, 6(5), e20419.

Camacho-Coronel, X., Molina-Torres, J. & Heil, M. (2020) Sequestration of exogenous volatiles by plant cuticular waxes as a mechanism of

passive associational resistance: a proof of concept. *Frontiers in Plant Science*, 11, 121.

Campa, A., Giraldez, R. & Ferreira, J.J. (2009) Genetic dissection of the resistance to nine anthracnose races in the common bean differential cultivars MDRK and TU. *Theoretical and Applied Genetics*, 119(1), 1–11.

Campa, A., Murube, E. & Ferreira, J. (2017) INTROGRESSION OF A POWDERY MILDEW RESISTANCE GENE INTO MARKET CLASS FABADA.

Campos, L., Granell, P., Tárraga, S., López-Gresa, P., Conejero, V., Bellés, J.M. et al. (2014) Salicylic acid and gentisic acid induce RNA silencing-related genes and plant resistance to RNA pathogens. *Plant Physiology and Biochemistry*, 77, 35–43.

Cappellin, L., Loreto, F., Biasioli, F., Pastore, P. & McKinney, K. (2019) A mechanism for biogenic production and emission of MEK from MVK decoupled from isoprene biosynthesis. *Atmospheric Chemistry and Physics*, 19(5), 3125–3135.

Castellanos-Ramos, J., Guzman-Maldonado, H., Kelly, J. & Acosta-Gallegos, J. (2003) Registration of 'Flor de Junio Marcela' common bean. (Registrations Of Cultivars). *Crop Science*, 43(3), 1121–1123.

Castillo, M.C., Martínez, C., Buchala, A., Métraux, J.-P. & León, J. (2004) Gene-specific involvement of β-oxidation in wound-activated responses in Arabidopsis. *Plant Physiology*, 135(1), 85–94.

Castro-Guerrero, N.A., Isidra-Arellano, M.C., Mendoza-Cozatl, D.G. & Valdés-López, O. (2016) Common bean: a legume model on the rise for unraveling responses and adaptations to iron, zinc, and phosphate deficiencies. *Frontiers in Plant Science*, 7, 600.

Cellini, A., Buriani, G., Rocchi, L., Rondelli, E., Savioli, S., Rodriguez Estrada, M.T. et al. (2018) Biological relevance of volatile organic compounds emitted during the pathogenic interactions between apple plants and Erwinia amylovora. *Molecular Plant Pathology*, 19(1), 158–168.

Chen, S., Zhang, L., Cai, X., Li, X., Bian, L., Luo, Z. et al. (2020) (E)-Nerolidol is a volatile signal that induces defenses against insects and pathogens in tea plants. *Horticulture Research*, 7(1), 1–15.

Chong, J., Soufan, O., Li, C., Caraus, I., Li, S., Bourque, G. et al. (2018) MetaboAnalyst 4.0: towards more transparent and integrative metabolomics analysis. *Nucleic Acids Research*, 46(W1), W486–W494.

Copolovici, L., Kännaste, A., Remmel, T. & Niinemets, Ü. (2014) Volatile organic compound emissions from Alnus glutinosa under interacting drought and herbivory stresses. *Environmental and Experimental Botany*, 100, 55–63.

Coppola, M., Cascone, P., Madonna, V., Di Lelio, I., Esposito, F., Avitabile, C. et al. (2017) Plant-to-plant communication triggered by systemin primes anti-herbivore resistance in tomato. *Scientific Reports*, 7(1), 1–13.

De Meyer, G., Audenaert, K. & Höfte, M. (1999) Pseudomonas aeruginosa 7NSK2-induced systemic resistance in tobacco depends on in planta salicylic acid accumulation but is not associated with PR1a expression. *European Journal of Plant Pathology*, 105(5), 513–517.

Di Piero, R.M. & Garda, M.V. (2008) Quitosana reduz a severidade da antracnose e aumenta a atividade de glucanase em feijoeiro-comum. *Pesquisa Agropecuária Brasileira*, 43(9), 1121–1128.

Ding, P. & Ding, Y. (2020) Stories of salicylic acid: a plant defense hormone. *Trends in Plant Science*, 25(6), 549–565.

Domingo, G., Marsoni, M., Chiodaroli, L., Fortunato, S., Bracale, M., De Pinto, M.C. et al. (2023) Quantitative phosphoproteomics reveals novel roles of cAMP in plants. *Proteomics*, 23, 2300165. Available from: https://doi.org/10.1002/pmic.202300165

Domingo, G., Vannini, C., Marsoni, M., Costantini, E., Bracale, M. & Di Iorio, A. (2023) A multifaceted approach to reveal the very-fine root's response of Fagus sylvatica seedlings to different drought intensities. *Physiologia Plantarum*, 175(3), e13934. Available from: https://doi.org/10.1111/ppl.13934

Doncheva, N.T., Morris, J.H., Gorodkin, J. & Jensen, L.J. (2018) Cytoscape StringApp: network analysis and visualization of proteomics data. *Journal of Proteome Research*, 18(2), 623–632.

Dudareva, N., Negre, F., Nagegowda, D.A. & Orlova, I. (2006) Plant volatiles: recent advances and future perspectives. *Critical Reviews in Plant Sciences*, 25(5), 417–440.

Eberl, F., Hammerbacher, A., Gershenzon, J. & Unsicker, S.B. (2018) Leaf rust infection reduces herbivore-induced volatile emission in black poplar and attracts a generalist herbivore. *New Phytologist*, 220(3), 760–772.

Escamilla-Treviño, L.L., Chen, W., Card, M.L., Shih, M.-C., Cheng, C.-L. & Poulton, J.E. (2006) *Arabidopsis thaliana* β-glucosidases BGLU45 and BGLU46 hydrolyse monolignol glucosides. *Phytochemistry*, 67(15), 1651–1660.

Fahey, J.W., Zalcmann, A.T. & Talalay, P. (2001) The chemical diversity and distribution of glucosinolates and isothiocyanates among plants. *Phytochemistry*, 56(1), 5–51.

Fall, R. (2003) Abundant oxygenates in the atmosphere: a biochemical perspective. *Chemical Reviews*, 103(12), 4941–4952.

Fichman, Y. & Mittler, R. (2020) Rapid systemic signaling during abiotic and biotic stresses: is the ROS wave master of all trades? *The Plant Journal*, 102(5), 887–896.

Flor, H. (1955) Host-parasite interactions in flax rust-its genetics and other implications. *Phytopathology*, 45, 680–685.

Fujisaki, K. & Ishikawa, M. (2008) Identification of an *Arabidopsis thaliana* protein that binds to tomato mosaic virus genomic RNA and inhibits its multiplication. *Virology*, 380(2), 402–411.

Ghosh, S., Malukani, K.K., Chandan, R.K., Sonti, R.V. & Jha, G. (2019) How plants respond to pathogen attack: interaction and communication. In: *Sensory biology of plants*. Singapore: Springer, pp. 537–568.

Gille, S. & Pauly, M. (2012) O-acetylation of plant cell wall polysaccharides. *Frontiers in Plant Science*, 3, 12.

Girón-Calva, P.S., Molina-Torres, J. & Heil, M. (2012) Volatile dose and exposure time impact perception in neighboring plants. *Journal of Chemical Ecology*, 38(2), 226–228.

Goh, H.H., Khairudin, K., Sukiran, N.A., Normah, M. & Baharum, S. (2016) Metabolite profiling reveals temperature effects on the VOC s and flavonoids of different plant populations. *Plant Biology*, 18, 130–139.

González, B. & Vera, P. (2019) Folate metabolism interferes with plant immunity through 1C methionine synthase-directed genome-wide DNA methylation enhancement. *Molecular Plant*, 12(9), 1227–1242.

Gorelova, V., Ambach, L., Rébeillé, F., Stove, C. & Van Der Straeten, D. (2017) Folates in plants: research advances and progress in crop biofortification. *Frontiers in Chemistry*, 5, 21.

Gorman, Z., Christensen, S.A., Yan, Y., He, Y., Borrego, E. & Kolomiets, M.V. (2020) Green leaf volatiles and jasmonic acid enhance susceptibility to anthracnose diseases caused by *Colletotrichum graminicola* in maize. *Molecular Plant Pathology*, 21(5), 702–715.

Han, M., Zhang, C., Suglo, P., Sun, S., Wang, M. & Su, T. (2021) l-Aspartate: an essential metabolite for plant growth and stress acclimation. *Molecules*, 26(7), 1887.

Hashimoto-Sugimoto, M., Higaki, T., Yaeno, T., Nagami, A., Irie, M., Fujimi, M. et al. (2013) A Munc13-like protein in Arabidopsis mediates H+-ATPase translocation that is essential for stomatal responses. *Nature Communications*, 4(1), 1–9.

Heil, M. (2014) Herbivore-induced plant volatiles: targets, perception and unanswered questions. *New Phytologist*, 204(2), 297–306.

Heil, M. & Bueno, J.C.S. (2007) Within-plant signaling by volatiles leads to induction and priming of an indirect plant defense in nature. *Proceedings of the National Academy of Sciences*, 104(13), 5467–5472.

Heil, M. & Kost, C. (2006) Priming of indirect defences. *Ecology Letters*, 9(7), 813–817.

Hochholdinger, F., Wen, T.J., Zimmermann, R., Chimot-Marolle, P., Da Costae Silva, O., Bruce, W. et al. (2008) The maize (Zea mays L.) roothairless3 gene encodes a putative GPI-anchored, monocot-specific, COBRA-like protein that significantly affects grain yield. *The Plant Journal*, 54(5), 888–898.

Holopainen, J.K. & Gershenzon, J. (2010) Multiple stress factors and the emission of plant VOCs. *Trends in Plant Science*, 15(3), 176–184.

Hooper, C.M., Castleden, I.R., Tanz, S.K., Aryamanesh, N. & Millar, A.H. (2017) SUBA4: the interactive data analysis Centre for Arabidopsis subcellular protein locations. *Nucleic Acids Research*, 45(D1), D1064–D1074.

Hou, S., Liu, Z., Shen, H. & Wu, D. (2019) Damage-associated molecular pattern-triggered immunity in plants. *Frontiers in Plant Science*, 10(646), 646.

Iriti, M. & Faoro, F. (2003) Benzothiadiazole (BTH) induces cell-death independent resistance in *Phaseolus vulgaris* against *Uromyces appendiculatus*. *Journal of Phytopathology*, 151(3), 171–180.

Jalakas, P., Huang, Y.-C., Yeh, Y.-H., Zimmerli, L., Merilo, E., Kollist, H. et al. (2017) The role of ENHANCED RESPONSES TO ABA1 (ERA1) in Arabidopsis stomatal responses is beyond ABA signaling. *Plant Physiology*, 174(2), 665–671.

Jewell, J.B. & Tanaka, K. (2019) Transcriptomic perspective on extracellular ATP signaling: a few curious trifles. *Plant Signaling & Behavior*, 14(11), 1659079.

Jones, J.D. & Dangl, J.L. (2006) The plant immune system. *Nature*, 444(7117), 323–329.

Jung, H.W., Panigrahi, G.K., Jung, G.Y., Lee, Y.J., Shin, K.H., Sahoo, A. et al. (2020) Pathogen-associated molecular pattern-triggered immunity involves proteolytic degradation of core nonsense-mediated mRNA decay factors during the early defense response. *The Plant Cell*, 32(4), 1081–1101.

Kalske, A., Shiojiri, K., Uesugi, A., Sakata, Y., Morrell, K. & Kessler, A. (2019) Insect herbivory selects for volatile-mediated plant-plant communication. *Current Biology*, 29(18), 3128–3133.e3.

Kelly, J.D. & Vallejo, V.A. (2004) A comprehensive review of the major genes conditioning resistance to anthracnose in common bean. *HortScience*, 39(6), 1196–1207.

Klessig, D.F., Choi, H.W. & Dempsey, D.M.A. (2018) Systemic acquired resistance and salicylic acid: past, present, and future. *Molecular Plant-Microbe Interactions*, 31(9), 871–888.

Koo, A.J., Chung, H.S., Kobayashi, Y. & Howe, G.A. (2006) Identification of a peroxisomal acyl-activating enzyme involved in the biosynthesis of jasmonic acid in Arabidopsis. *Journal of Biological Chemistry*, 281(44), 33511–33520.

Kost, C. & Heil, M. (2006) Herbivore-induced plant volatiles induce an indirect defence in neighbouring plants. *Journal of Ecology*, 94(3), 619–628.

Kourtchenko, O., Andersson, M.X., Hamberg, M., Brunnström, Å., Göbel, C., McPhail, K.L. et al. (2007) Oxo-phytodienoic acid-containing galactolipids in Arabidopsis: jasmonate signaling dependence. *Plant Physiology*, 145(4), 1658–1669.

Li, T., Holst, T., Michelsen, A. & Rinnan, R. (2019) Amplification of plant volatile defence against insect herbivory in a warming Arctic tundra. *Nature Plants*, 5(6), 568–574.

Lichtenthaler, H.K. (1999) The 1-deoxy-D-xylulose-5-phosphate pathway of isoprenoid biosynthesis in plants. *Annual Review of Plant Biology*, 50(1), 47–65.

Liu, F., Wei, F., Wang, L., Liu, H., Zhu, X. & Liang, Y. (2010) Riboflavin activates defense responses in tobacco and induces resistance against Phytophthora parasitica and Ralstonia solanacearum. *Physiological and Molecular Plant Pathology*, 74(5–6), 330–336.

Loreto, F., Barta, C., Brilli, F. & Nogues, I. (2006) On the induction of volatile organic compound emissions by plants as consequence of wounding or fluctuations of light and temperature. *Plant, Cell & Environment*, 29(9), 1820–1828.

Loreto, F. & Schnitzler, J.-P. (2010) Abiotic stresses and induced BVOCs. *Trends in Plant Science*, 15(3), 154–166.

Malekvia, S.D., Bell, T.L. & Adams, M.A. (2007) PTR-MS analysis of reference and plant-emitted volatile organic compounds. *International Journal of Mass Spectrometry*, 262(3), 203–210.

Matsui, K., Minami, A., Hornung, E., Shibata, H., Kishimoto, K., Ahnert, V. et al. (2006) Biosynthesis of fatty acid derived aldehydes is induced upon mechanical wounding and its products show fungicidal activities in cucumber. *Phytochemistry*, 67(7), 649–657.

Mohammed, A. (2013) An overview of distribution, biology and the management of common bean anthracnose. *Journal of Plant Pathology and Microbiology*, 4(8), 1–6.

Mungalu, H., Sansala, M., Hamabwe, S., Mukuma, C., Gepts, P., Kelly, J.D. et al. (2020) Identification of race-specific quantitative trait loci for resistance to *Colletotrichum lindemuthianum* in an Andean population of common bean. *Crop Science*, 60(6), 2843–2856.

Myers, J.R. & Kmiecik, K. (2017) Common bean: economic importance and relevance to biological science research. In: *The common bean genome*. Cham: Springer, pp. 1–20.

Nunes, M.P.B.A., Gonçalves-Vidigal, M.C., Martins, V.S.R., Xavier, L.F.S., Valentini, G., Vaz Bisneta, M. et al. (2021) Relationship of *Colletotrichum lindemuthianum* races and resistance loci in the *Phaseolus vulgaris* L. genome. *Crop Science*, 61(6), 3877–3893.

Oblessuc, P.R., Borges, A., Chowdhury, B., Caldas, D.G.G., Tsai, S.M., Camargo, L.E.A. et al. (2012) Dissecting *Phaseolus vulgaris* innate immune system against *Colletotrichum lindemuthianum* infection. *PLoS One*, 7(8), e43161.

Padder, B.A., Kamfwa, K., Awale, H.E. & Kelly, J.D. (2016) Transcriptome profiling of the *Phaseolus vulgaris-Colletotrichum lindemuthianum* pathosystem. *PLoS One*, 11(11), e0165823.

Paradiso, A., Domingo, G., Blanco, E., Buscaglia, A., Fortunato, S., Marsoni, M. et al. (2020) Cyclic AMP mediates heat stress response by the control of redox homeostasis and ubiquitin-proteasome system. *Plant, Cell & Environment*, 43(11), 2727–2742.

Perez-Riverol, Y., Csordas, A., Bai, J., Bernal-Llinares, M., Hewapathirana, S., Kundu, D.J. et al. (2019) The PRIDE database and related tools and resources in 2019: improving support for quantification data. *Nucleic Acids Research*, 47(D1), D442–D450.

Pieterse, C.M., Van der Does, D., Zamioudis, C., Leon-Reyes, A. & Van Wees, S.C. (2012) Hormonal modulation of plant immunity. *Annual Review of Cell and Developmental Biology*, 28, 489–521.

Pinfield-Wells, H., Rylott, E.L., Gilday, A.D., Graham, S., Job, K., Larson, T.R. et al. (2005) Sucrose rescues seedling establishment but not germination of Arabidopsis mutants disrupted in peroxisomal fatty acid catabolism. *The Plant Journal*, 43(6), 861–872.

Portillo-Estrada, M., Okereke, C.N., Jiang, Y., Talts, E., Kaurilind, E. & Niinemets, Ü. (2021) Wounding-induced VOC emissions in five tropical agricultural species. *Molecules*, 26(9), 2602.

Prats, E., Gay, A.P., Mur, L.A.J., Thomas, B.J. & Carver, T.L.W. (2006) Stomatal lock-open, a consequence of epidermal cell death, follows transient suppression of stomatal opening in barley attacked by Blumeria graminis. *Journal of Experimental Botany*, 57(10), 2211–2226.

Quintana-Rodriguez, E., Morales-Vargas, A.T., Molina-Torres, J., Ádame-Alvarez, R.M., Acosta-Gallegos, J.A. & Heil, M. (2015) Plant volatiles cause direct, induced and associational resistance in common bean to the fungal pathogen C olletotrichum lindemuthianum. *Journal of Ecology*, 103(1), 250–260.

Quintana-Rodriguez, E., Rivera-Macias, L.E., Adame-Alvarez, R.M., Torres, J.M. & Heil, M. (2018) Shared weapons in fungus-fungus and fungus-plant interactions? Volatile organic compounds of plant or fungal origin exert direct antifungal activity in vitro. *Fungal Ecology*, 33, 115–121.

Ren, D., Yang, H. & Zhang, S. (2002) Cell death mediated by MAPK is associated with hydrogen peroxide production in Arabidopsis. *Journal of Biological Chemistry*, 277(1), 559–565.

Rendón-Anaya, M., Montero-Vargas, J.M., Saburido-Álvarez, S., Vlasova, A., Capella-Gutierrez, S., Ordaz-Ortiz, J.J. et al. (2017) Genomic history of the origin and domestication of common bean unveils its closest sister species. *Genome Biology*, 18(1), 1–17.

Rippa, M., Pasqualini, A., Curcio, R., Mormile, P. & Pane, C. (2023) Active vs. passive thermal imaging for helping the early detection of soil-borne rot diseases on wild rocket [*Diplotaxis tenuifolia* (L.) D.C.]. *Plants (Basel)*, 12(8), 1615.

Robert-Seilaniantz, A., Grant, M. & Jones, J.D. (2011) Hormone crosstalk in plant disease and defense: more than just jasmonate-salicylate antagonism. *Annual Review of Phytopathology*, 49, 317–343.

Sakr, S., Wang, M., Dédaldéchamp, F., Perez-Garcia, M.-D., Ogé, L., Hamama, L. et al. (2018) The sugar-signaling hub: overview of regulators and interaction with the hormonal and metabolic network. *International Journal of Molecular Sciences*, 19(9), 2506.

Schilmiller, A.L., Koo, A.J. & Howe, G.A. (2007) Functional diversification of acyl-coenzyme A oxidases in jasmonic acid biosynthesis and action. *Plant Physiology*, 143(2), 812–824.

Sharma, P., Sharma, O., Padder, B. & Kapil, R. (2008) Yield loss assessment in common bean due to anthracnose (*Colletotrichum lindemuthianum*) under sub temperate conditions of North-Western Himalayas. *Indian Phytopathology*, 61(3), 323.

Shi, C., Baldwin, I.T. & Wu, J. (2012) Arabidopsis plants having defects in nonsense-mediated mRNA decay factors UPF1, UPF2, and UPF3 show photoperiod-dependent phenotypes in development and stress responses. *Journal of Integrative Plant Biology*, 54(2), 99–114.

Sicard, D., Michalakis, Y., Dron, M. & Neema, C. (1997) Genetic diversity and pathogenic variation of *Colletotrichum lindemuthianum* in the three centers of diversity of its host, *Phaseolus vulgaris*. *Phytopathology*, 87(8), 807–813.

Siegrist, J., Orober, M. & Buchenauer, H. (2000) β-Aminobutyric acid-mediated enhancement of resistance in tobacco to tobacco mosaic virus depends on the accumulation of salicylic acid. *Physiological and Molecular Plant Pathology*, 56(3), 95–106.

Singh, P. & Pandey, A.K. (2021) Dysphania ambrosioides essential oils: from pharmacological agents to uses in modern crop protection—a review. *Phytochemistry Reviews*, 21, 1–19.

Song, G.C. & Ryu, C.-M. (2013) Two volatile organic compounds trigger plant self-defense against a bacterial pathogen and a sucking insect in cucumber under open field conditions. *International Journal of Molecular Sciences*, 14(5), 9803–9819.

Sulkowska, A., Auber, A., Sikorski, P.J., Silhavy, D., Auth, M., Sitkiewicz, E. et al. (2020) RNA helicases from the DEA (D/H)-box family contribute to plant NMD efficiency. *Plant and Cell Physiology*, 61(1), 144–157.

Szklarczyk, D., Franceschini, A., Wyder, S., Forslund, K., Heller, D., Huerta-Cepas, J. et al. (2015) STRING v10: protein–protein interaction networks, integrated over the tree of life. *Nucleic Acids Research*, 43(D1), D447–D452.

Taheri, P. & Tarighi, S. (2011) A survey on basal resistance and riboflavin-induced defense responses of sugar beet against *Rhizoctonia solani*. *Journal of Plant Physiology*, 168(10), 1114–1122.

Takemiya, A., Sugiyama, N., Fujimoto, H., Tsutsumi, T., Yamauchi, S., Hiyama, A. et al. (2013) Phosphorylation of BLUS1 kinase by phototropins is a primary step in stomatal opening. *Nature Communications*, 4(1), 1–8.

Tanaka, K. & Heil, M. (2021) Damage-associated molecular patterns (DAMPs) in plant innate immunity: applying the danger model and evolutionary perspectives. *Annual Review of Phytopathology*, 59, 53–75.

Ul Hassan, M.N., Zainal, Z. & Ismail, I. (2015) Green leaf volatiles: biosynthesis, biological functions and their applications in biotechnology. *Plant Biotechnology Journal*, 13(6), 727–739.

Vannini, C., Marsoni, M., Scoccianti, V., Ceccarini, C., Domingo, G., Bracale, M. et al. (2019) Proteasome-mediated remodeling of the proteome and phosphoproteome during kiwifruit pollen germination. *Journal of Proteomics*, 192, 334–345.

Venice, F., Chialva, M., Domingo, G., Novero, M., Carpentieri, A., Salvioli di Fossalunga, A. et al. (2021) Symbiotic responses of *Lotus japonicus* to two isogenic lines of a mycorrhizal fungus differing in the presence/absence of an endobacterium. *The Plant Journal*, 108(6), 1547–1564. Available from: https://doi.org/10.1111/tpj.15578

Ventura, I., Brunello, L., Iacopino, S., Valeri, M.C., Novi, G., Dornbusch, T. et al. (2020) Arabidopsis phenotyping reveals the importance of alcohol dehydrogenase and pyruvate decarboxylase for aerobic plant growth. *Scientific Reports*, 10(1), 1–14.

Verhage, A., van Wees, S.C. & Pieterse, C.M. (2010) Plant immunity: it's the hormones talking, but what do they say? *Plant Physiology*, 154(2), 536–540.

von Caemmerer, S. & Farquhar, G.D. (1981) Some relationships between the biochemistry of photosynthesis and the gas exchange of leaves. *Planta*, 153(4), 376–387.

Wang, Y., Yang, L., Chen, X., Ye, T., Zhong, B., Liu, R. et al. (2016) Major latex protein-like protein 43 (MLP43) functions as a positive regulator during abscisic acid responses and confers drought tolerance in *Arabidopsis thaliana*. *Journal of Experimental Botany*, 67(1), 421–434.

Wheatley, R., Hackett, C., Bruce, A. & Kundzewicz, A. (1997) Effect of substrate composition on production of volatile organic compounds from Trichoderma spp. inhibitory to wood decay fungi. *International Biodeterioration & Biodegradation*, 39(2–3), 199–205.

Wilkins, K. (1996) Volatile metabolites from actinomycetes. *Chemosphere*, 32(7), 1427–1434.

Winter, G., Todd, C.D., Trovato, M., Forlani, G. & Funck, D. (2015) Physiological implications of arginine metabolism in plants. *Frontiers in Plant Science*, 6, 534.

Yáñez-Serrano, A.M., Nölscher, A.C., Bourtsoukidis, E., Derstroff, B., Zannoni, N., Gros, V. et al. (2016) Atmospheric mixing ratios of methyl ethyl ketone (2-butanone) in tropical, boreal, temperate and marine environments. *Atmospheric Chemistry and Physics*, 16(17), 10965–10984.

Yi, H.-S., Heil, M., Adame-Alvarez, R.M., Ballhorn, D.J. & Ryu, C.-M. (2009) Airborne induction and priming of plant defenses against a bacterial pathogen. *Plant Physiology*, 151(4), 2152–2161.

Zhang, S., Yang, X., Sun, M., Sun, F., Deng, S. & Dong, H. (2009) Riboflavin-induced priming for pathogen defense in *Arabidopsis thaliana*. *Journal of Integrative Plant Biology*, 51(2), 167–174.

Zheng, Z., Nonomura, T., Appiano, M., Pavan, S., Matsuda, Y., Toyoda, H. et al. (2013) Loss of function in Mlo orthologs reduces susceptibility of pepper and tomato to powdery mildew disease caused by *Leveillula taurica*. *PLoS One*, 8(7), e70723.

SUPPORTING INFORMATION

Additional supporting information can be found online in the Supporting Information section at the end of this article.